

Supplementary Materials

Mesoscale Assembly of Bisteroidal Esters from Terephthalic Acid

Gabriel Guerrero-Luna,¹ María Guadalupe Hernández-Linares,^{2,3*} Sylvain Bernès,⁴ Alan Carrasco-Carballo,¹ Diana Montalvo-Guerrero,⁵ María A. Fernández-Herrera,⁵ Jesús Sandoval-Ramírez.¹

¹*Facultad de Ciencias Químicas. Benemérita Universidad Autónoma de Puebla. 72570 Puebla, Pue., México. jesus.sandoval@correo.buap.mx; gabriel.guerrero@alumno.buap.mx; alan.carballo@alumno.buap.mx*

²*Centro de Química. Instituto de Ciencias. Benemérita Universidad Autónoma de Puebla. 72570 Puebla, Pue., México. guadalupe.mgħl@correo.buap.mx*

³*Laboratorio de Investigación. Herbario y Jardín Botánico Universitario. Benemérita Universidad Autónoma de Puebla. 72570 Puebla, Pue., México.*

⁴*Instituto de Física. Benemérita Universidad Autónoma de Puebla. 72570 Puebla, Pue., México. Sylvain_bernes@hotmail.com*

⁵*Departamento de Física Aplicada. Centro de Investigación y de Estudios Avanzados - Unidad Mérida, km 6 Antigua Carretera a Progreso, Cordemex, 97310 Mérida, Yuc., México. mfernandez@cinvestav.mx, diana.montalvo@cinvestav.mx*

*Correspondence: e-mail: guadalupe.mgħl@correo.buap.mx; Tel/fax 52222295500 e7039.

Table of contents

Figures of DSC, TGA, IR, ^1H NMR, ^{13}C NMR, 2D-NMR and MS spectra of compounds.	
Figure S1. IR spectrum of the Bicholesterol ester (5).....	4
Figure S2. Mass spectrum of Bicholesterol ester (5).....	4
Figure S3. ^{13}C NMR spectrum at 125 MHz in CDCl_3 of Bicholesterol ester (5).....	5
Figure S4. Differential scanning calorimetry (DSC) of Bicholesterol ester (5).....	5
Figure S5. ^1H NMR spectrum at 500 MHz in CDCl_3 of Bicholestanol ester (6).....	6
Figure S6. ^{13}C NMR spectrum at 125 MHz in CDCl_3 of the of Bicholestanol ester (6).....	7
Figure S7. HSQC-NMR spectrum at 500 MHz of Bicholestanol ester (6).....	7
Figure S8. IR spectrum of Bidiosgenin ester (8a).....	8
Figure S9. HRMS data of Bidiosgenin ester (8a).....	8
Figure S10. HSQC-NMR spectrum at 500 MHz in CDCl_3 of Bidiosgenin ester (8a).....	9
Figure S11. Thermogravimetric analysis of Bidiosgenin ester (8a).....	9
Figure S12. IR spectrum of Bihecogenin ester (8b).....	10
Figure S13. Mass spectrum of Bihecogenin ester (8b).....	10
Figure S14. ^1H -NMR spectrum at 500 MHz in CDCl_3 of Bihecogenin ester (8b).....	11
Figure S15. ^{13}C -NMR spectrum at 125 MHz in CDCl_3 of Bihecogenin ester (8b).....	11
Figure S16. Differential Scanning Calorimetry analysis of Bihecogenin ester (8b).....	12
Figure S17. IR spectrum of Bisarsasapogenin ester (8c).....	13
Figure S18. ^1H -NMR spectrum at 500 MHz in CDCl_3 of Bisarsasapogenin ester (8c).....	13
Figure S19. ^{13}C -NMR spectrum at 125 MHz in CDCl_3 of Bisarsasapogenin ester (8c).....	14
Figure S20. HSQC-NMR spectrum at 500 MHz in CDCl_3 of Bisarsasapogenin ester (8c).....	14
Figure S21. Differential Scanning Calorimetry analysis of Bisarsasapogenin ester (8c).....	15
Figure S22. IR spectrum of Bi-23-acetyldiosgenin ester (10a).....	15
Figure S23. Mass spectrum data of Bi-23-acetyldiosgenin ester (10a).....	16
Figure S24. ^1H -NMR spectrum at 500 MHz in CDCl_3 of Bi-23-acetyldiosgenin ester (10a).....	16
Figure S25. ^{13}C -NMR spectrum at 125 MHz in CDCl_3 of Bi-23-acetyldiosgenin ester (10a).....	17
Figure S26. HSQC-NMR spectrum at 500 MHz in CDCl_3 of Bi-23-acetyldiosgenin ester (10a).....	17
Figure S27. HMBC-NMR spectrum in CDCl_3 of Bi-23-acetyldiosgenin ester (10a).....	18
Figure S28. Differential Scanning Calorimetry analysis of Bi-23-acetyldiosgenin ester (10a).....	18
Figure S29. IR spectrum of Bi-23-acetylhecogenin ester (10b).....	19

Figure S30. Mass spectrum of Bi-23-acetylhecogenin ester (10b).....	19
Figure S31. HSQC-NMR spectrum at 500 MHz of Bi-23-acetylhecogenin ester (10b).....	20
Figure S32. COSY-NMR spectrum at 500 MHz of Bi-23-acetylhecogenin ester (10b).....	20
Figure S33. Differential Scanning Calorimetry analysis of Bi-23-acetylhecogenin ester (10b).....	21
Figure S34. Molecular structure with MM2 energy minimization method for 6 and 8c	21

Figures of SEM images of compounds.

Figure S35 Bicholesterol ester (5) in hexane/ EtOAc	22
Figure S36 Bicholesterol ester (5) in hexane/ EtOAc	22
Figure S37. Bicholesterol ester (5) EtOAc	23
Figure S38. Bidiosgenin ester (8a) in EtOAc	23
Figure S39. Bidiosgenin ester (8a) in CHCl ₃ /MeOH.....	24
Figure S40. Bidiosgenin ester (8a) in CHCl ₃ /MeOH.....	24
Figure S41. Bisarsasapogenin ester (8c) in hexane/EtOAc.....	25
Figure S42. Bi-23-acetyldiosgenin ester (10a) in EtOAc	25
Figure S43. Bi-23-acetyldiosgenin ester (10a) in EtOAc.....	26
Figure S44. Bi-23-acetyldiosgenin ester (10a) in EtOAc.....	26
Figure S45. Bi-23-acetylhecogenin ester (10b) in EtOAc.....	27
Figure S46. Bi-23-acetylhecogenin ester (10b) in EtOAc.....	27

Powder X-Ray Diffraction (PXRD) analysis.

Figure S47. PXRD patterns for raw materials of steroidal dimers 5 , 6 , 8c , 10a and 10b	28
Figure S48. Comparison of the X-ray diffraction patterns of bidiosgenin ester (8a) under different conditions: raw material, layered material, in contact with chloroform-methanol, and with hexane-ethyl acetate.....	28

Bicholesterol ester (**5**).

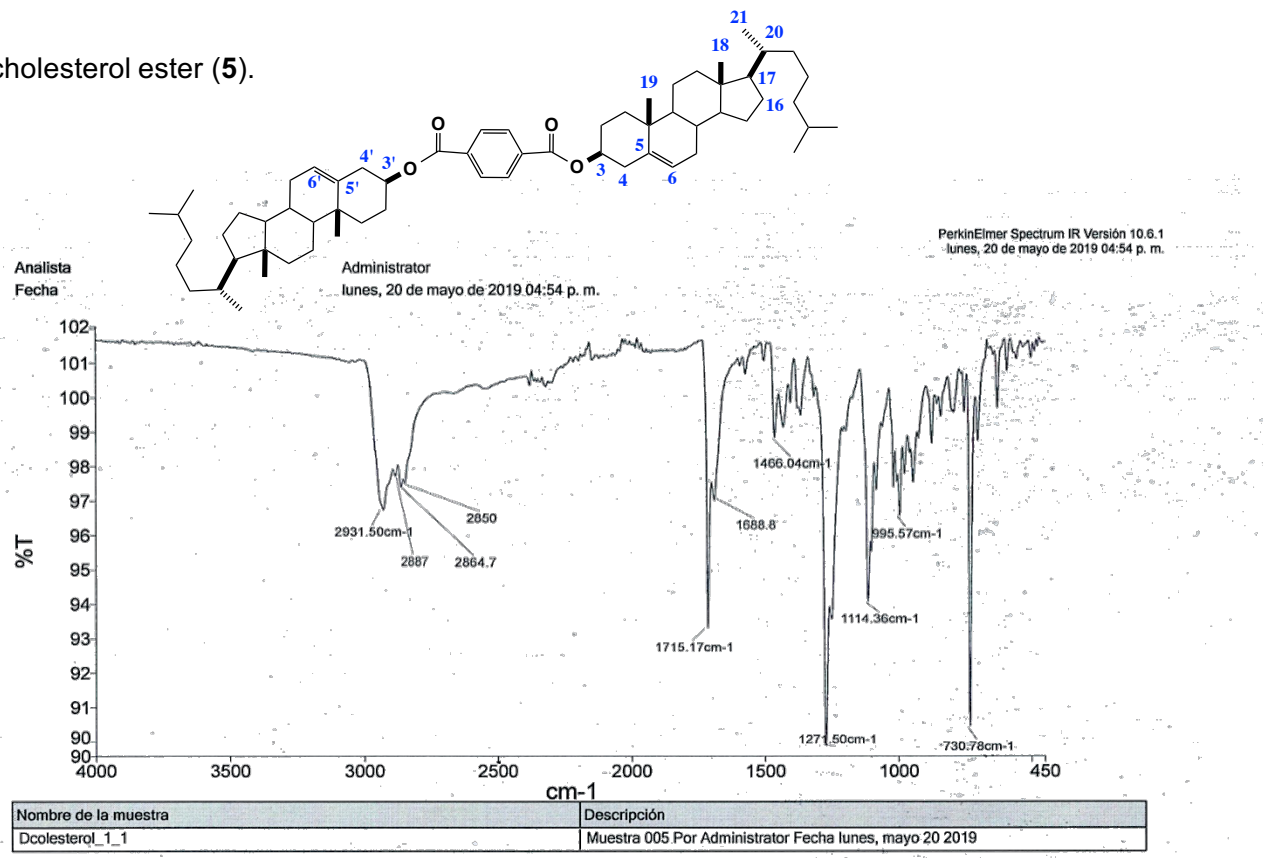


Figure S1. IR spectrum of Bicholesterol ester (**5**).

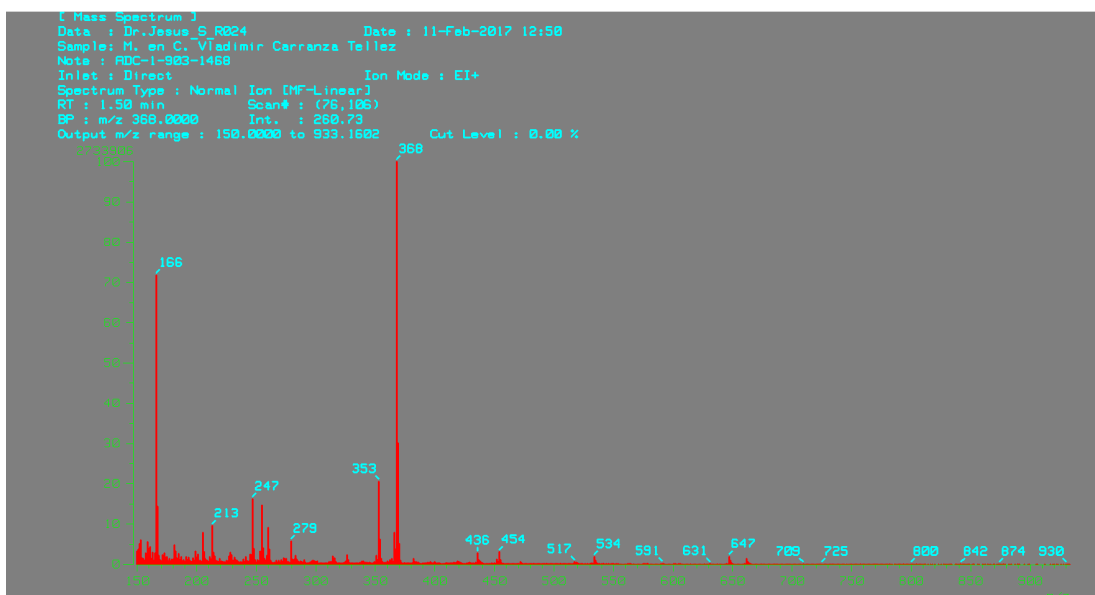


Figure S2. Mass spectrum of Bicholesterol ester (**5**).

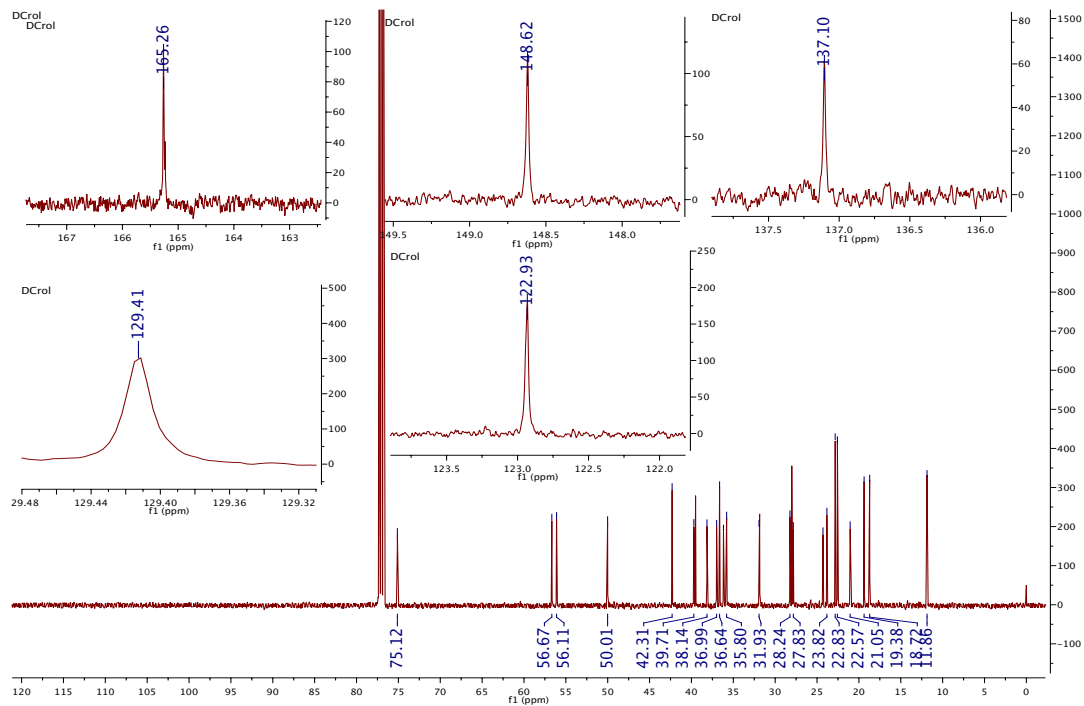


Figure S3. ^{13}C NMR spectrum at 125 MHz in CDCl_3 of Bicholesterol ester (**5**).

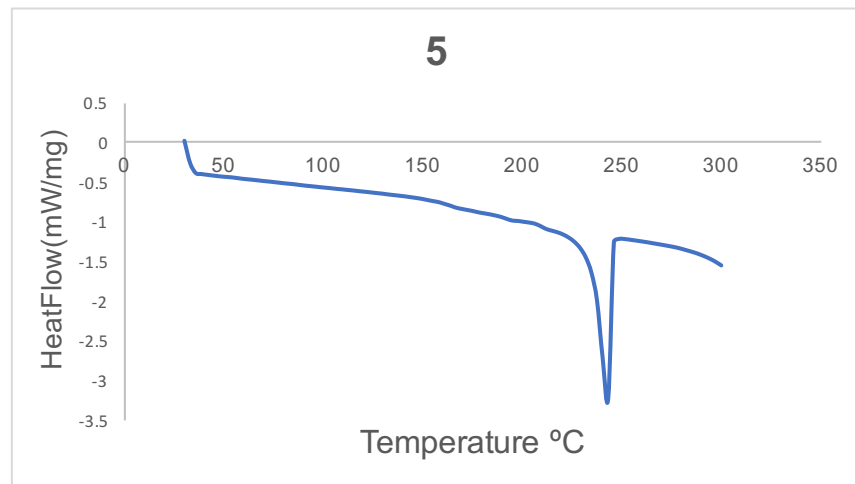


Figure S4. Differential scanning calorimetry (DSC) of Bicholesterol ester (**5**).

Bicholestanol ester (**6**)

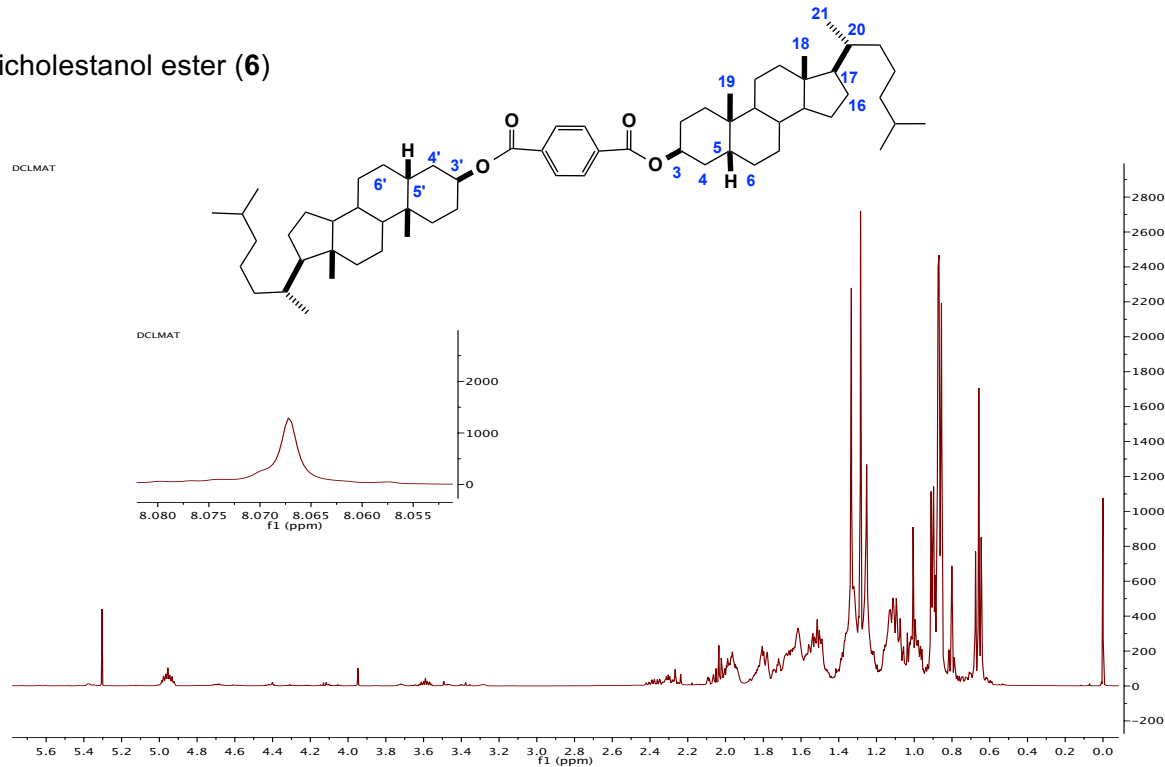


Figure S5. ^1H NMR spectrum at 500 MHz in CDCl_3 of Bicholestanol ester (**6**).

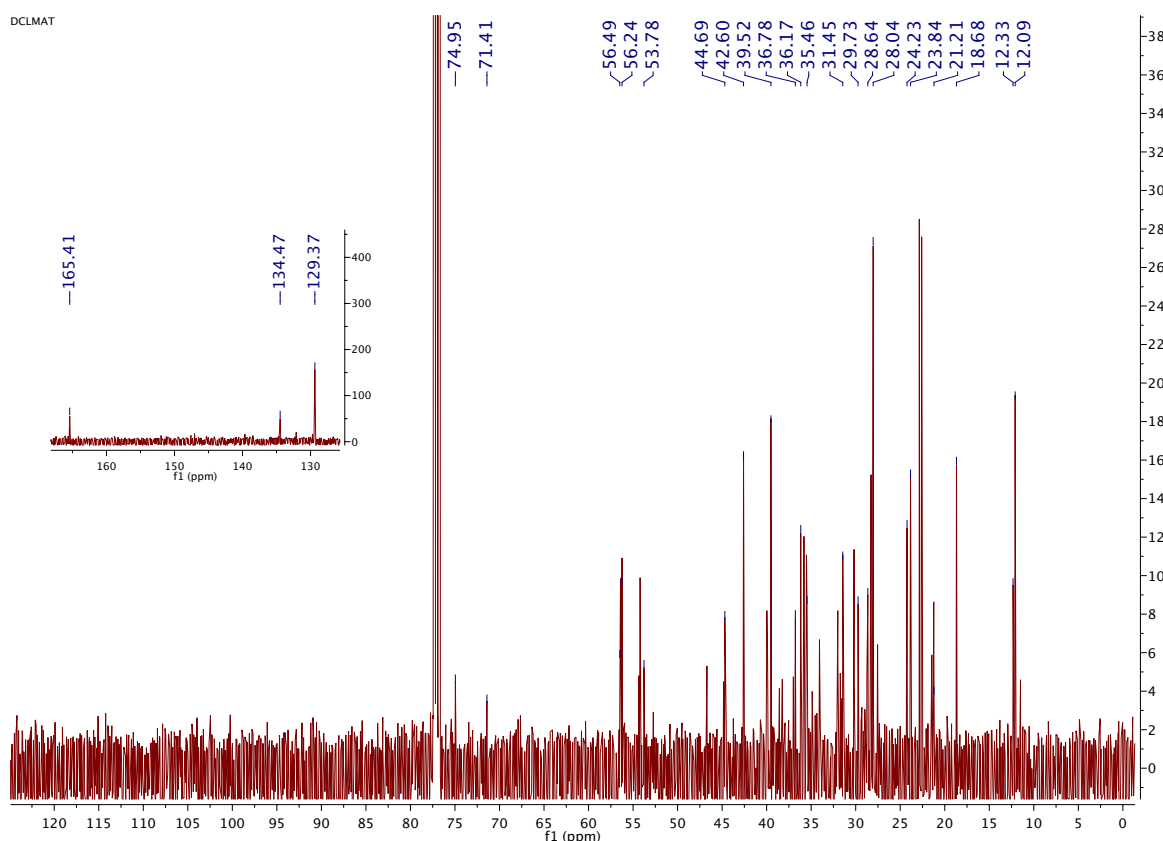


Figure S6. ^{13}C NMR spectrum at 125 MHz in CDCl_3 of the of Bicholestanol ester (**6**).

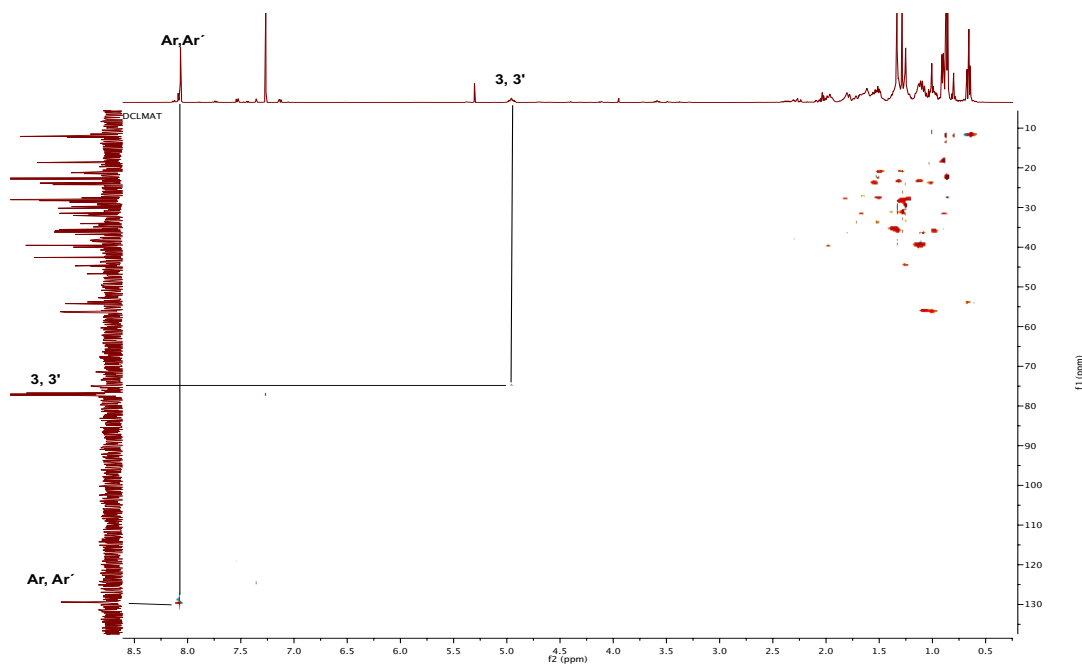


Figure S7. HSQC-NMR spectrum at 500 MHz of Bicholestanol ester (**6**).

Bidiosgenin terephthalate (**8a**).

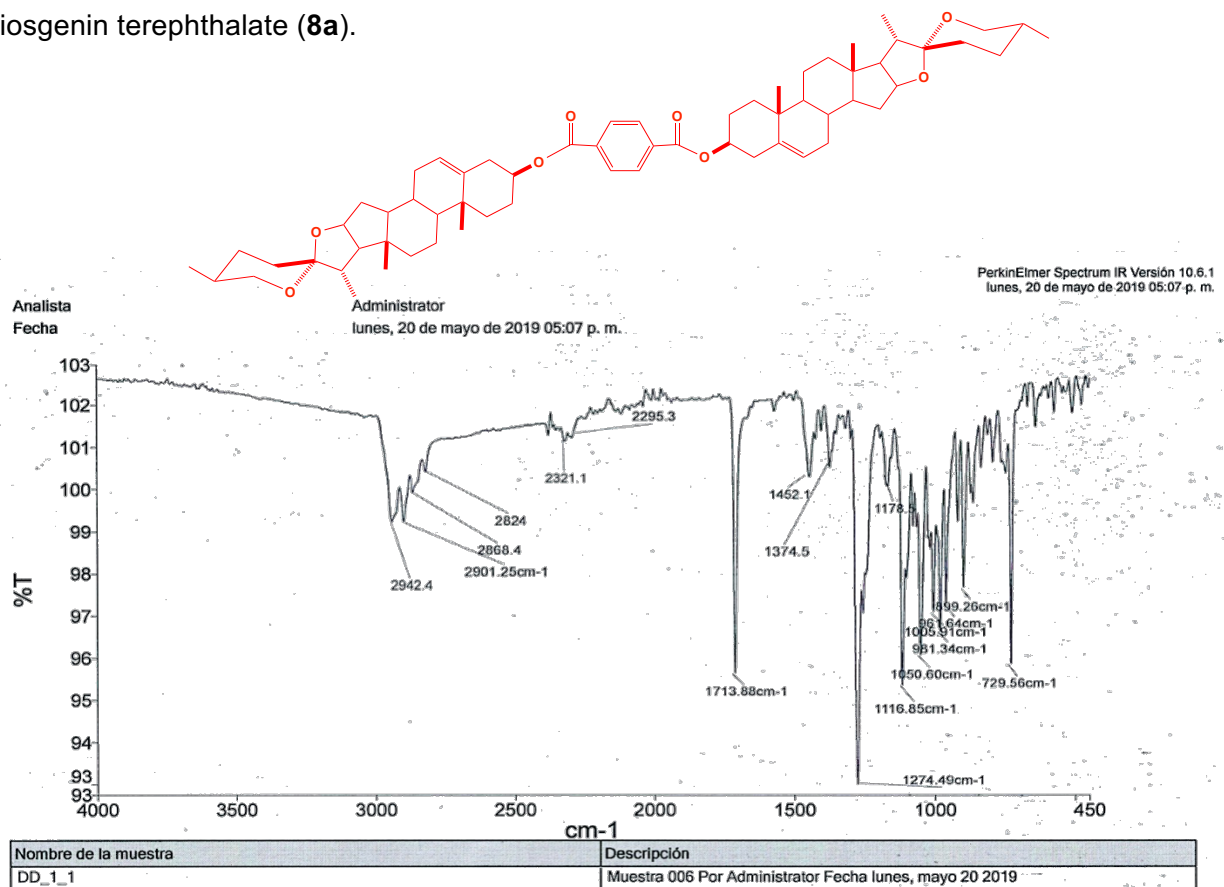


Figure S8. IR spectrum of Bidiosgenin ester (**8a**).

[Elemental Composition]
 Data : Dr-Jesus-Sandoval013
 Sample: STE-2215 LupDD
 Note : -
 Inlet : Direct Ion Mode : FAB+
 RT : 0.36 min Scan#: (1,6)
 Elements : C 64/0, H 120/0, O 28/0
 Mass Tolerance : 1000ppm, 2mmu if m/z > 2
 Unsaturation (U.S.) : -0.5 - 30.0

Observed m/z	Int%
959.6414	85.7

Estimated m/z	Error [ppm]	U.S.	C	H	O
959.6401	+1.4	19.5	62	87	8

Page: 1

Figure S9. HRMS data of Bidiosgenin ester (**8a**).

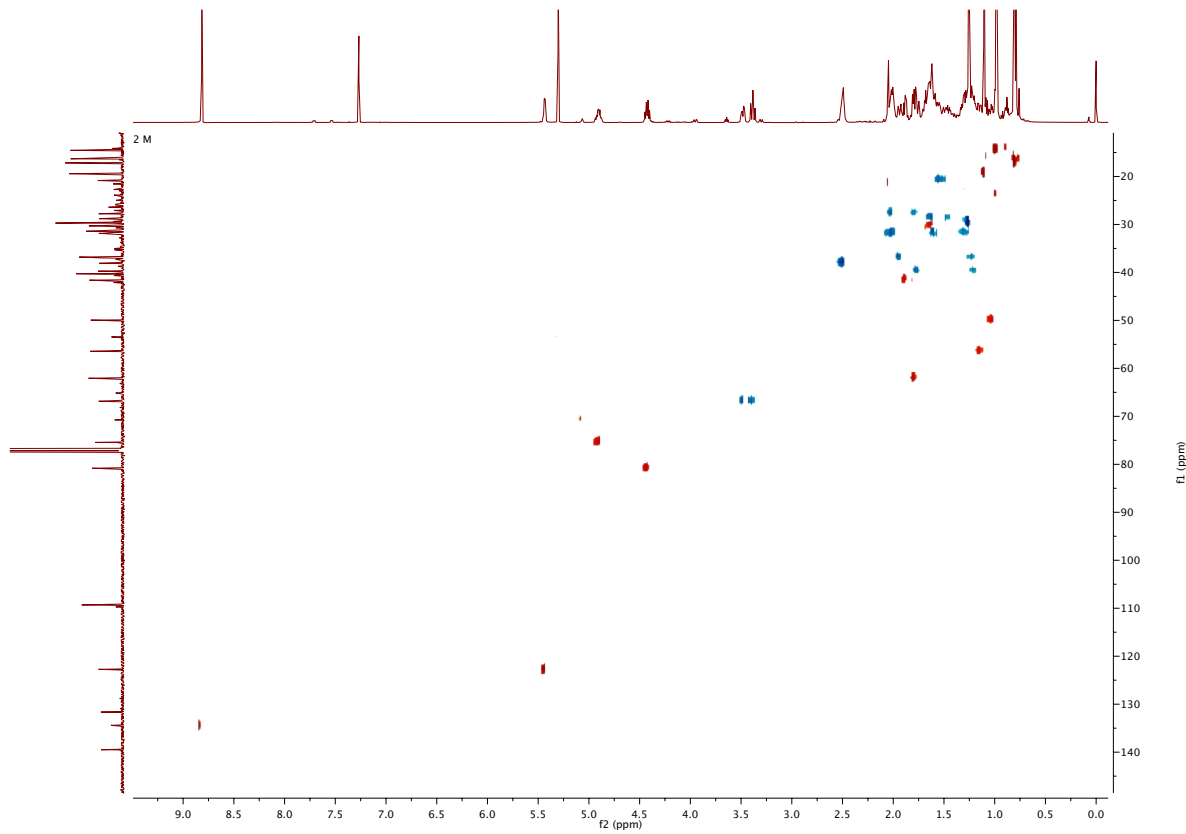


Figure S10. HSQC-NMR spectrum at 600 MHz in CDCl_3 of Bidiosgenin ester (**8a**).

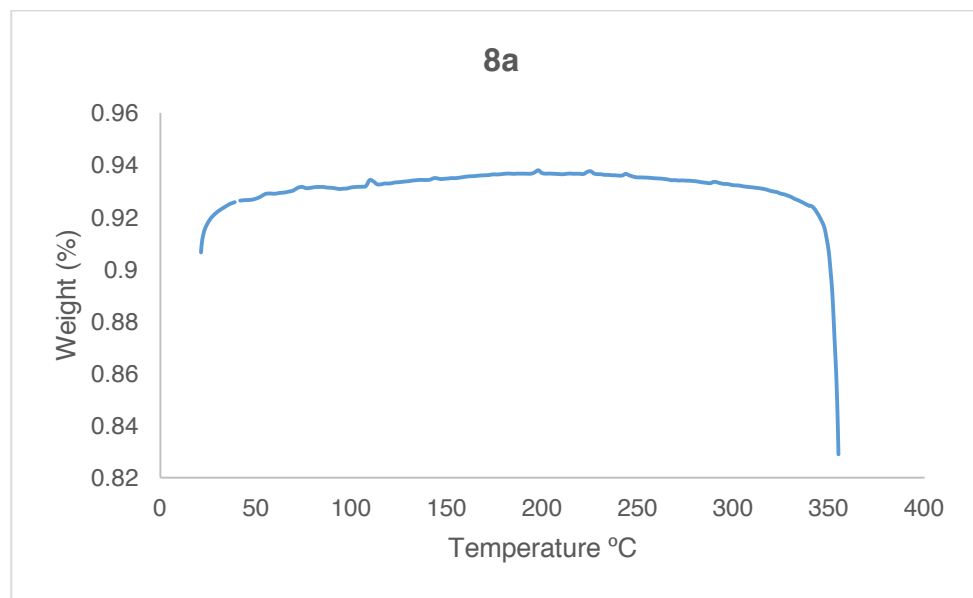


Figure S11. Thermogravimetric analysis of Bidiosgenin ester (**8a**).

Bihecogenin terephthalate (8b).

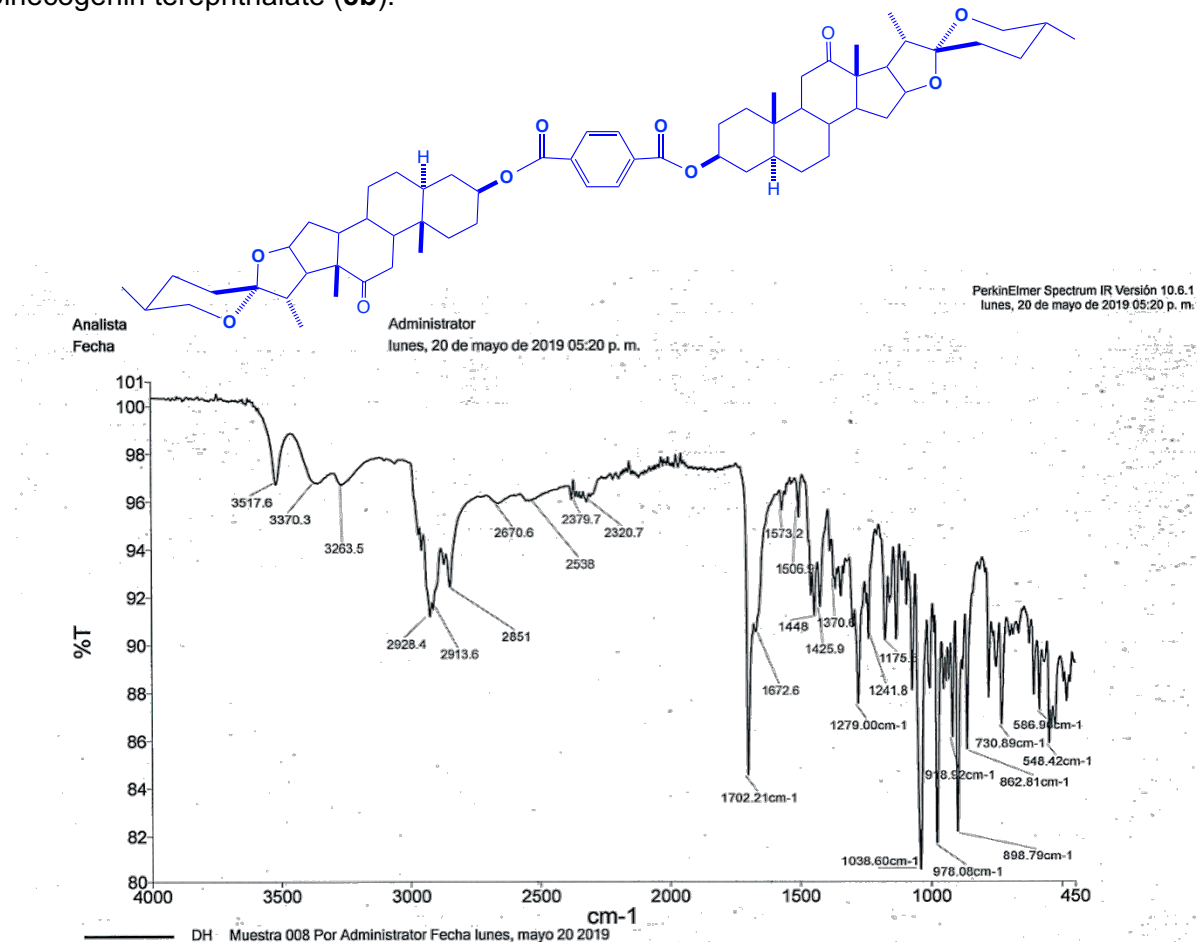


Figure S12. IR spectrum of Bihecogenin ester (8b).

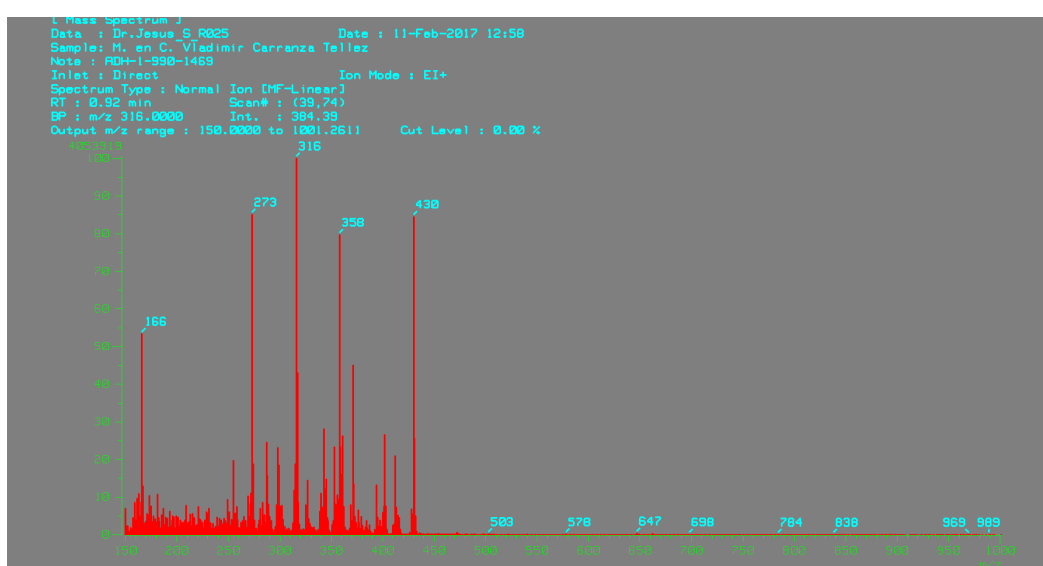
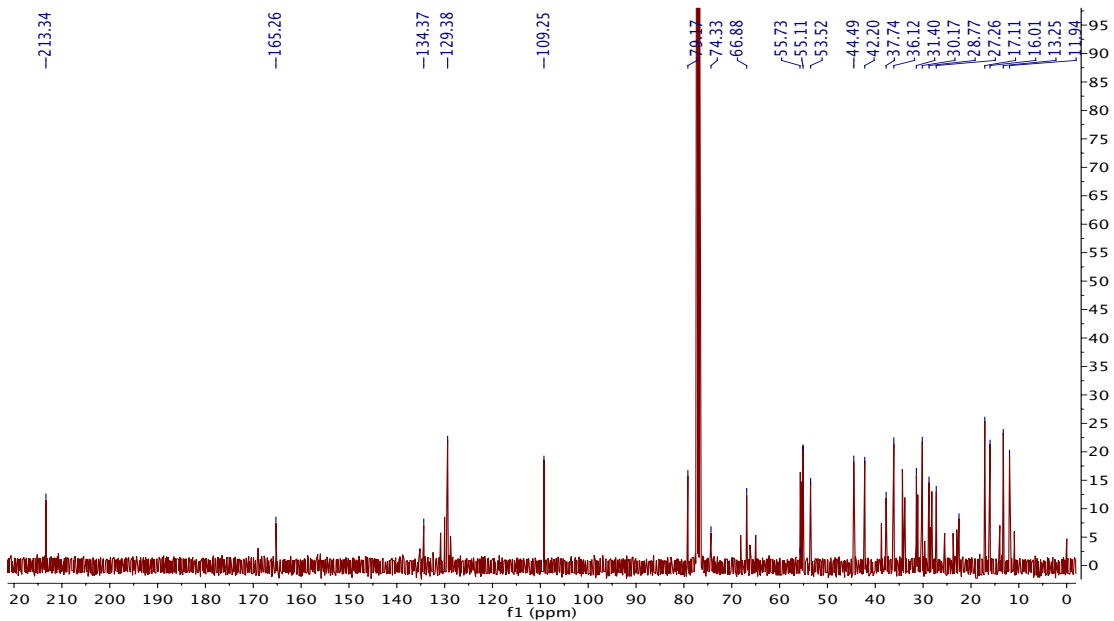
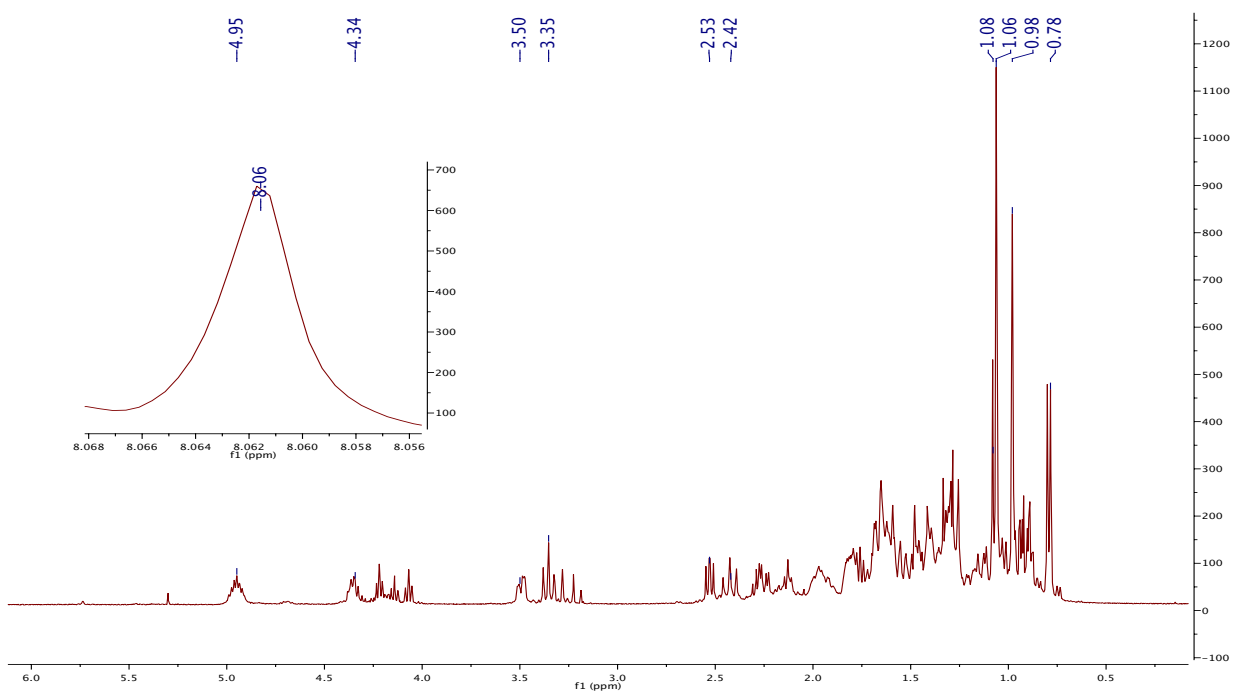


Figure S13. Mass spectrum of Bihecogenin ester (8b).



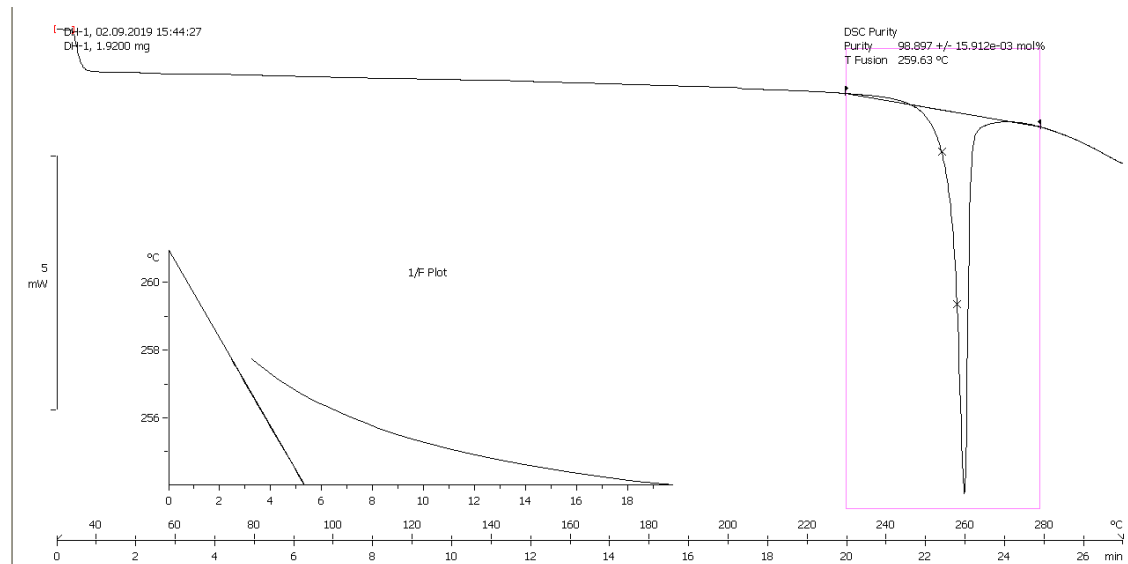


Figure S16. Differential Scanning Calorimetry analysis of Bihecogenin ester (**8b**).

Bisarsasapogenin terephthalate (**8c**)

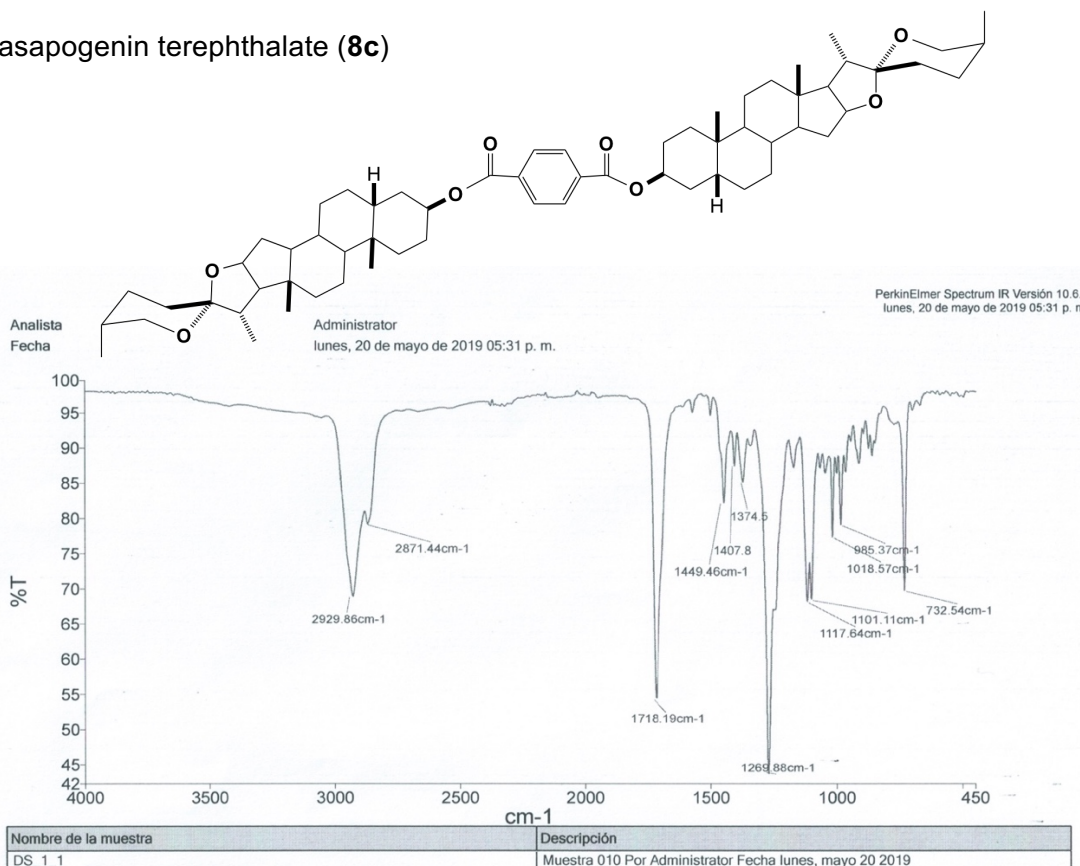


Figure S17. IR spectrum of Bisarsasapogenin ester (**8c**).

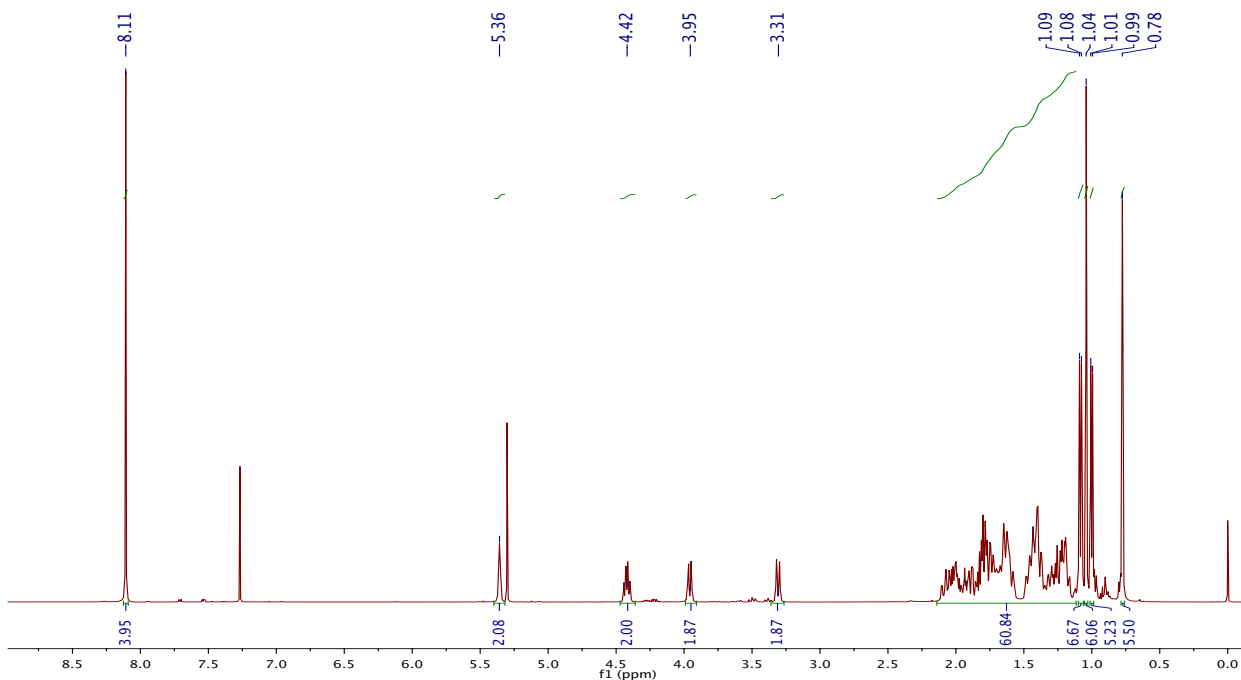


Figure S18. ¹H-NMR spectrum at 500 MHz in CDCl₃ of Bisarsasapogenin ester (**8c**).

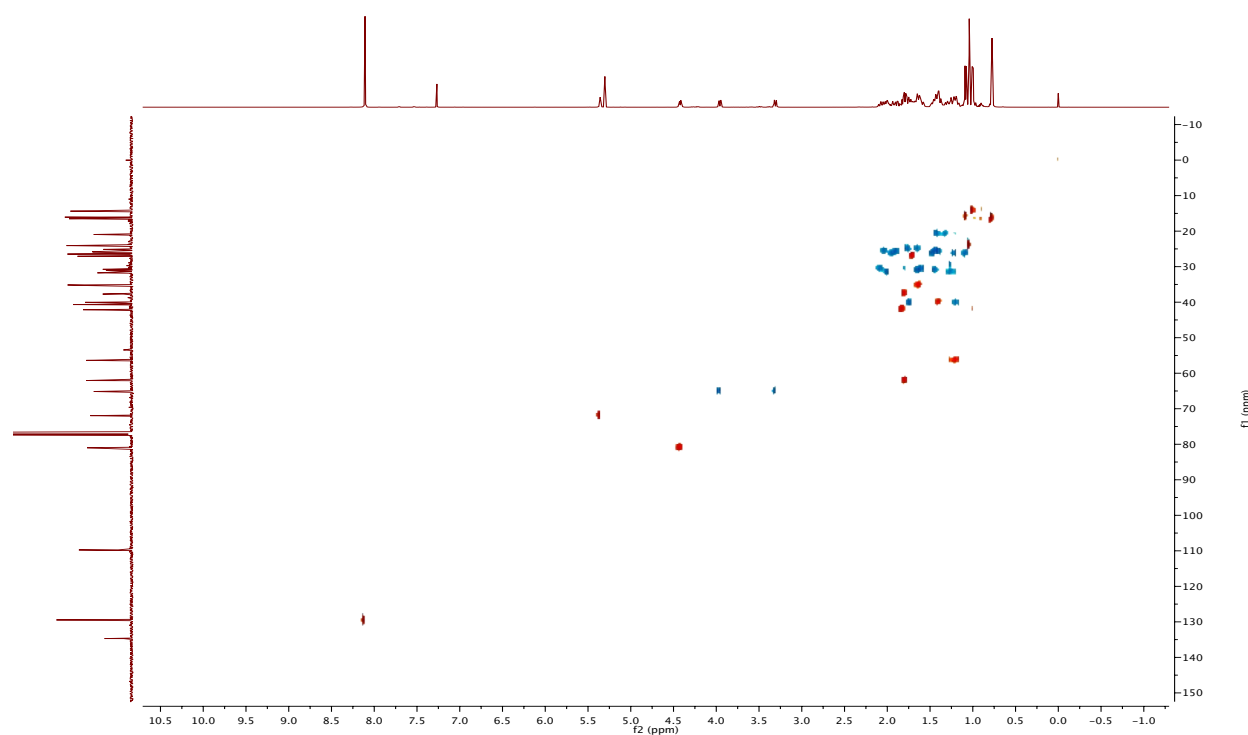
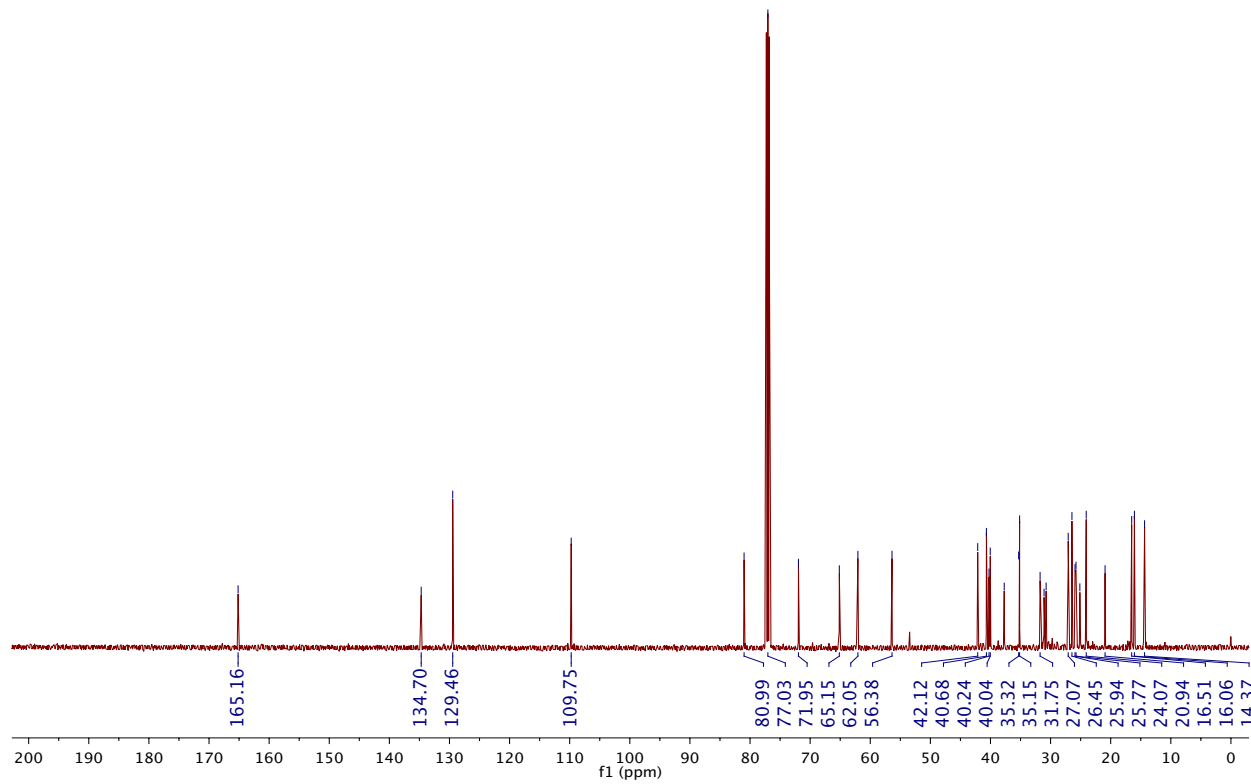


Figure S20. HSQC-NMR spectrum at 500 MHz in CDCl_3 of Bisarsasapogenin ester (**8c**).

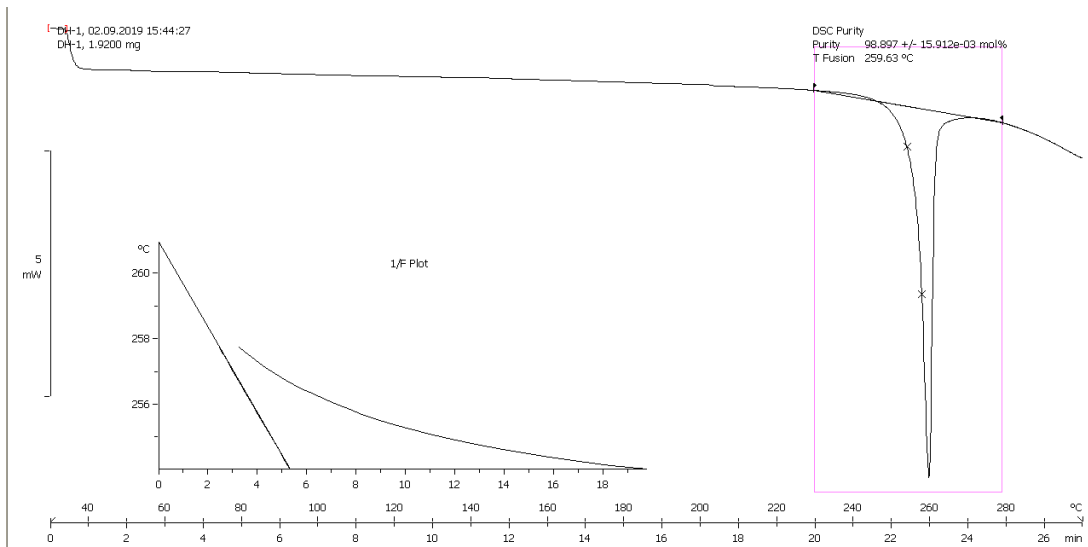


Figure S21. Differential Scanning Calorimetry analysis of Bisarsasapogenin ester (**8c**).

Bi-23-acetyldiosgenin terephthalate (10a).

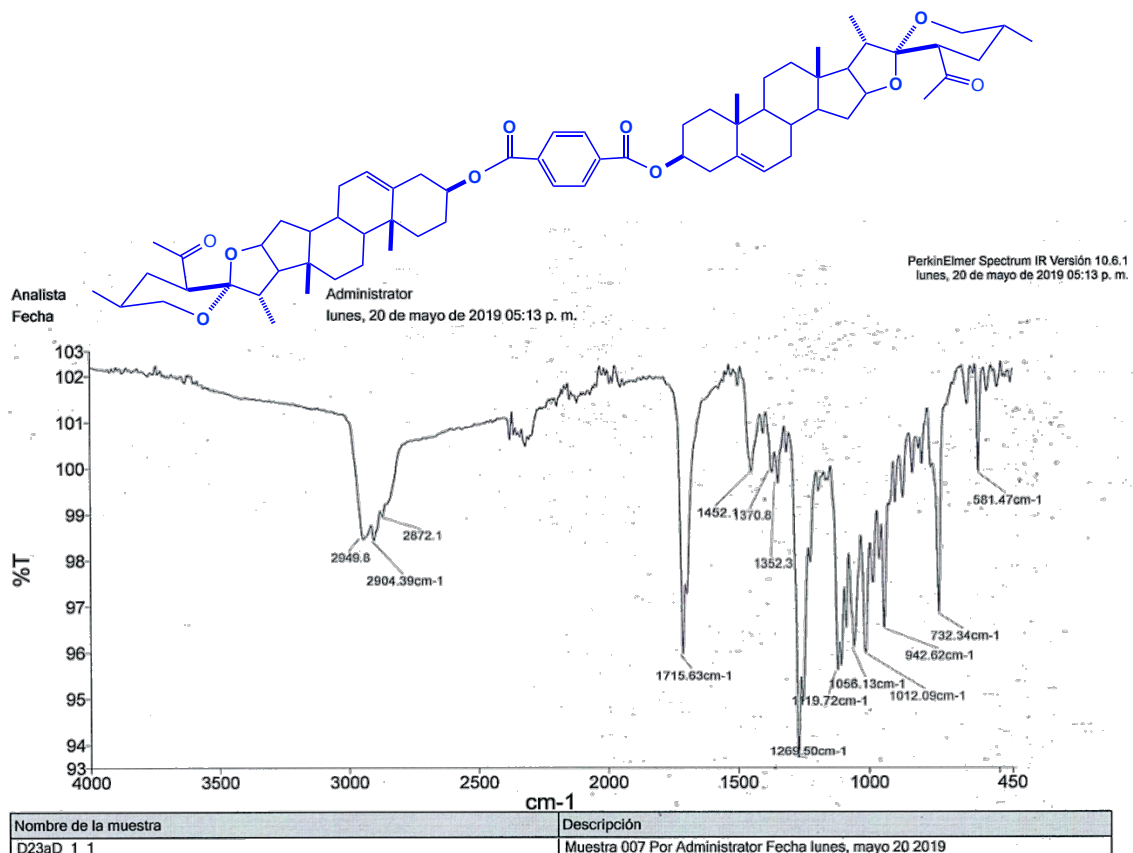


Figure S22. IR spectrum of Bi-23-acetyldiosgenin ester (**10a**).

[Elemental Composition]
 Data : Dr-Jesus-Sandoval039 Date : 08-Oct-2010 13:20
 Sample: 65-STE-2216 Lup-23aD
 Note : Luis-Velasco
 Inlet : Direct Ion Mode : FAB+
 RT : 9.15 min Scan# : (65, 76)
 Elements : C 70/1, H 95/1, O 12/1
 Mass Tolerance : 1000ppm, 2mmu if m/z > 2
 Unsaturation (U.S.) : 0.0 - 50.0

Observed m/z	Int%				
1043.6609	41.2				
Estimated m/z	Error [ppm]	U.S.	C	H	O
1043.6612	-0.3	21.5	66	91	10

Page: 1

Figure S23. Mass spectrum data of Bi-23-acetyldiosgenin ester (**10a**).

tmpstudy_data_PROTON_01
 MAF-D23aD

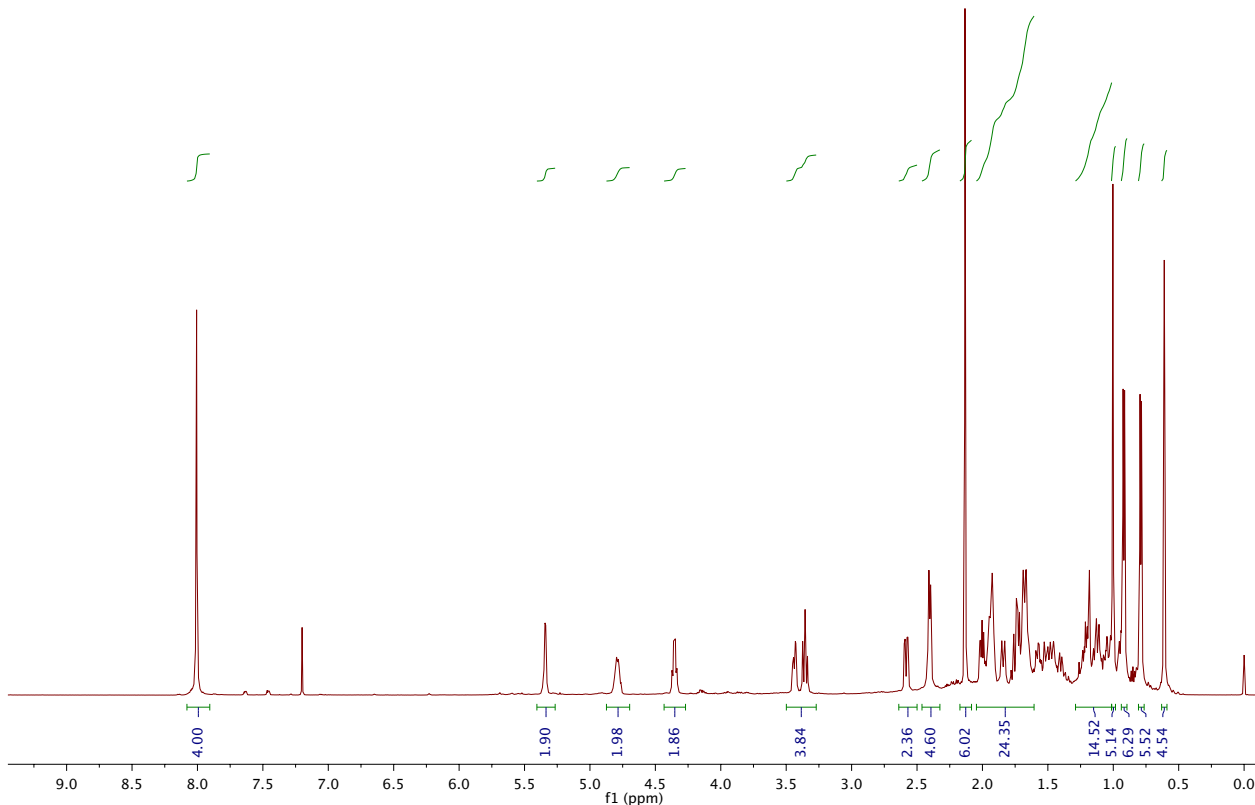


Figure S24. ^1H -NMR spectrum at 600 MHz in CDCl_3 of Bi-23-acetyldiosgenin ester (**10a**).

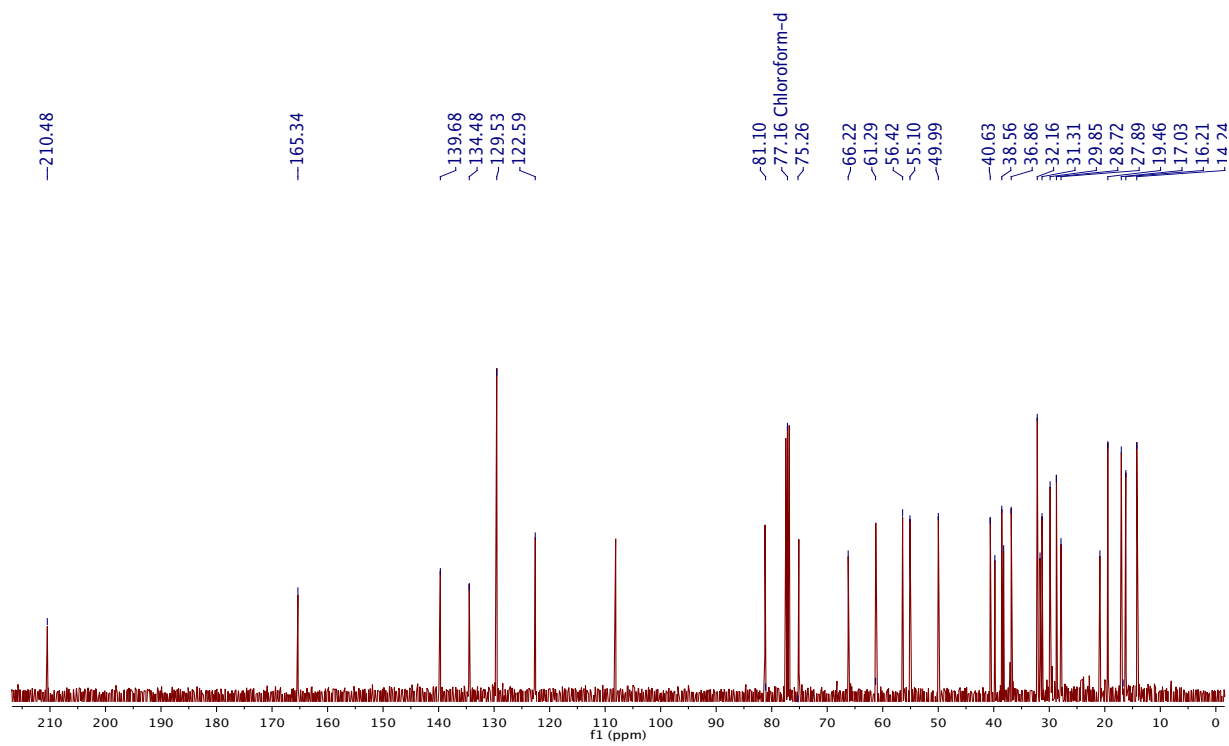


Figure S25. ^{13}C -NMR spectrum at 150 MHz in CDCl_3 of Bi-23-acetyldiosgenin ester (**10a**).

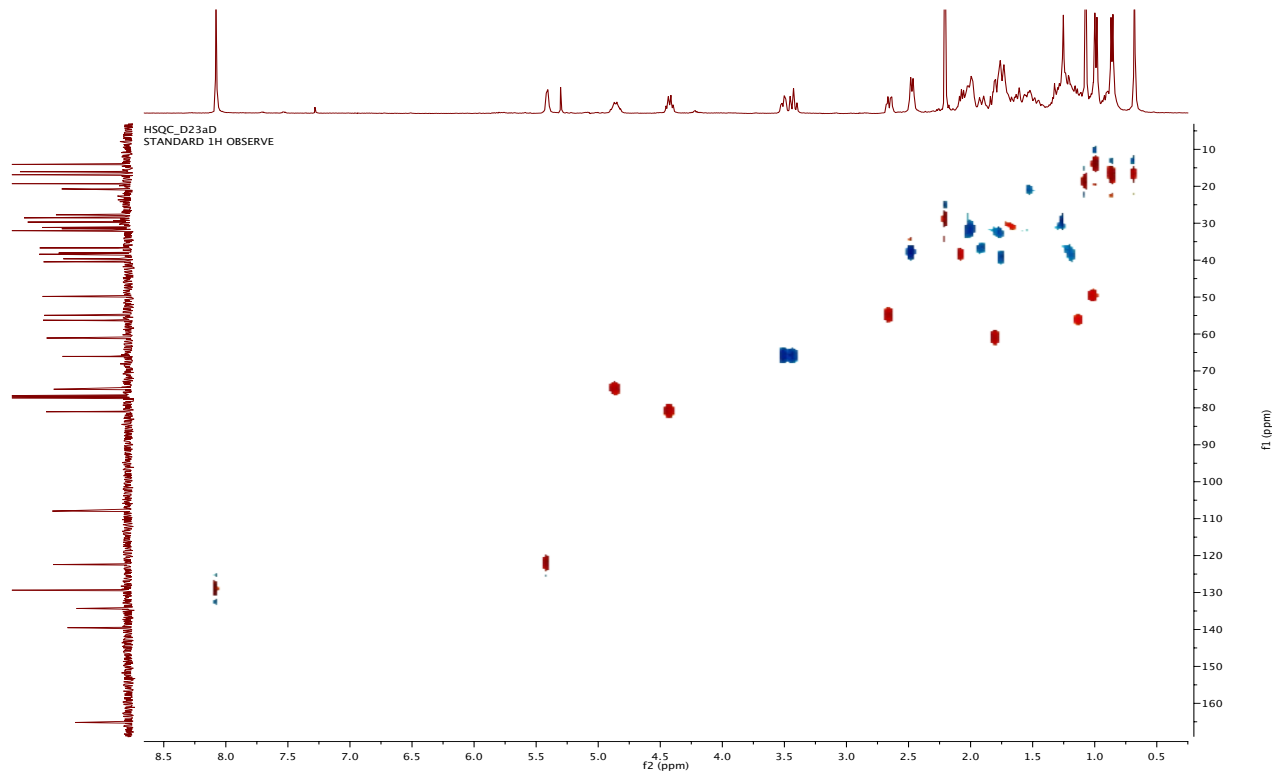


Figure S26. HSQC-NMR spectrum at 500 MHz in CDCl_3 of Bi-23-acetyldiosgenin ester (**10a**).

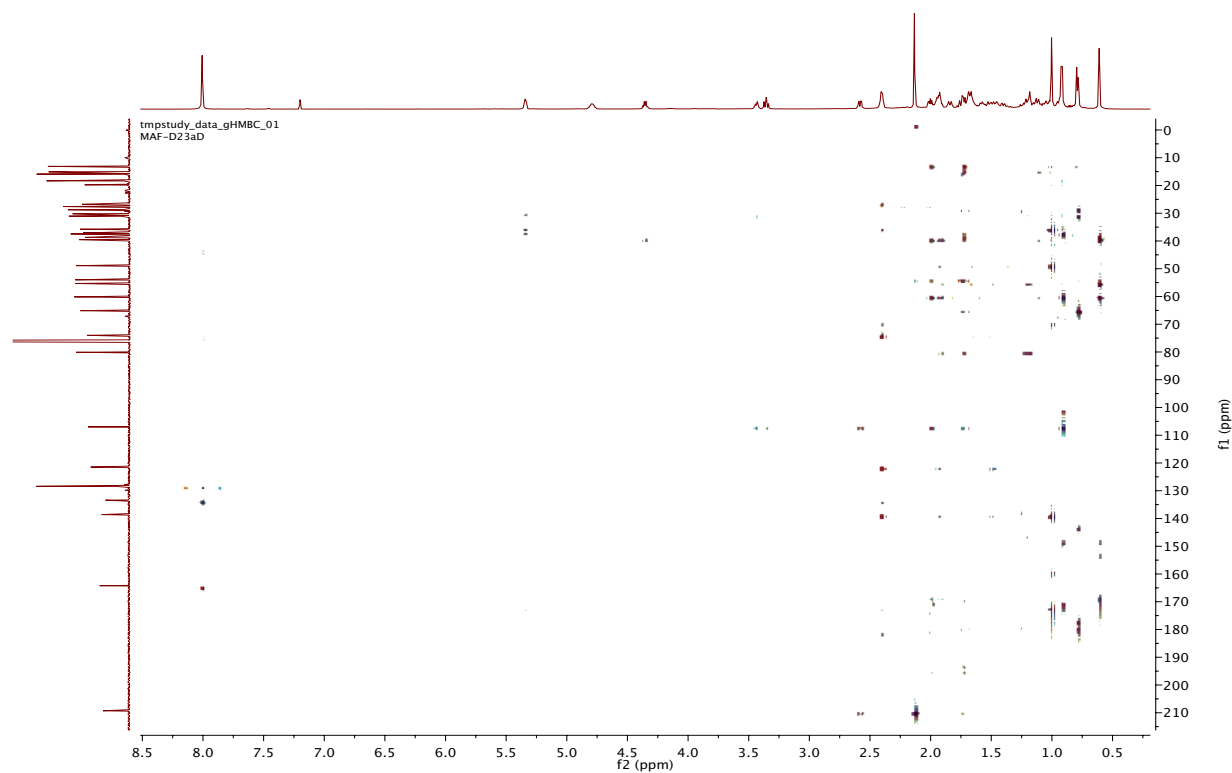


Figure S27. HMBC-NMR experiment al 600 MHz in CDCl_3 of Bi-23-acetyldiosgenin ester (**10a**).

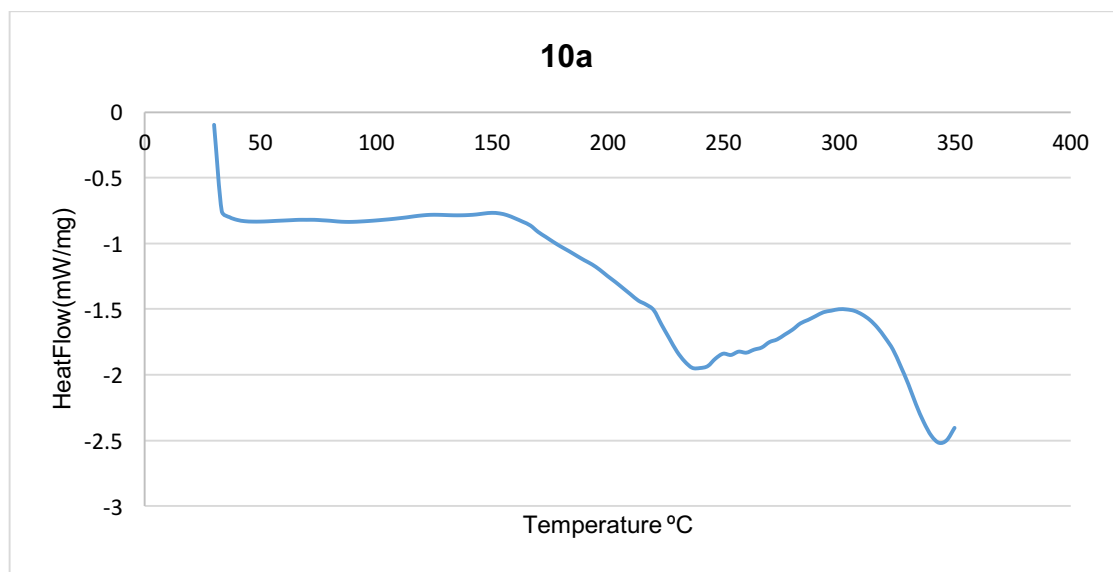


Figure S28. Differential Scanning Calorimetry analysis of Bi-23-acetyldiosgenin ester (**10a**).

Bi-23-acetylhecogenin terephthalate (10b).

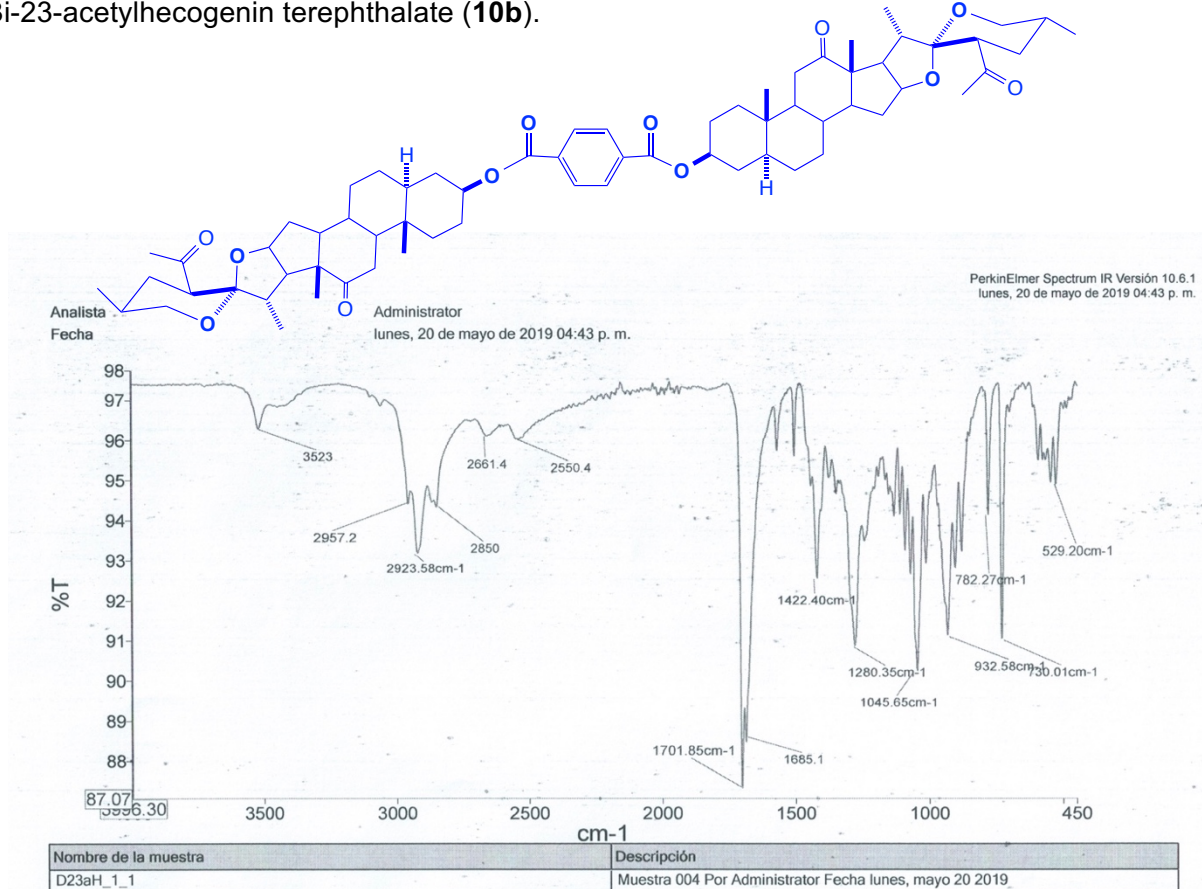


Figure S29. IR spectrum of Bi-23-acetylhecogenin ester (10b).

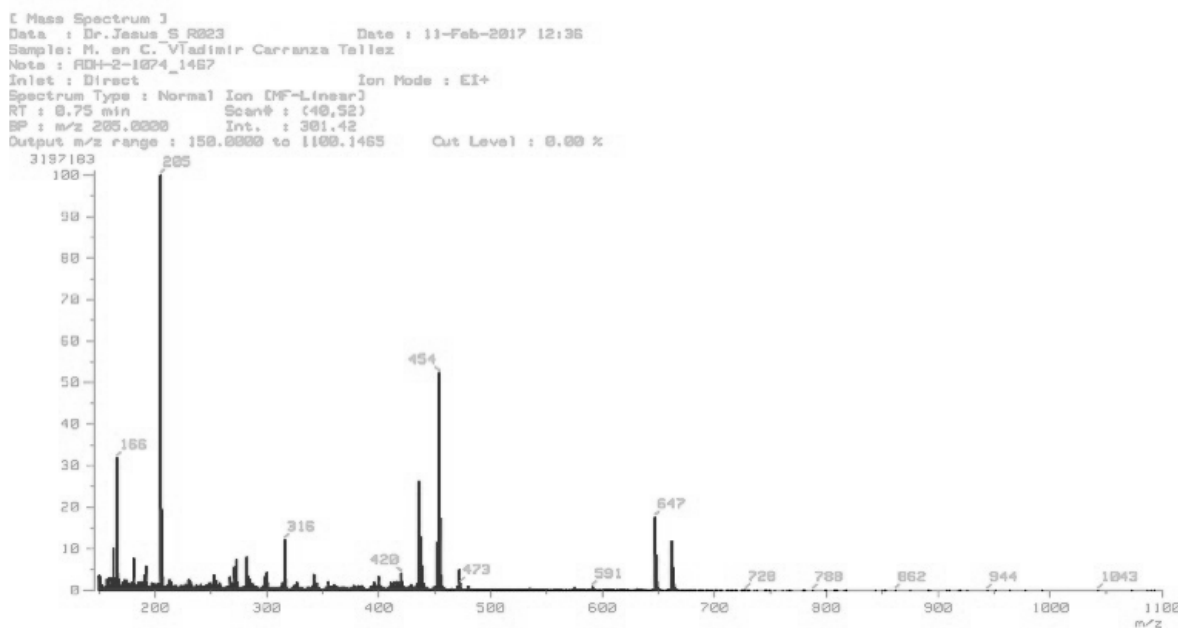


Figure S30. Mass spectrum of Bi-23-acetylhecogenin ester (10b).

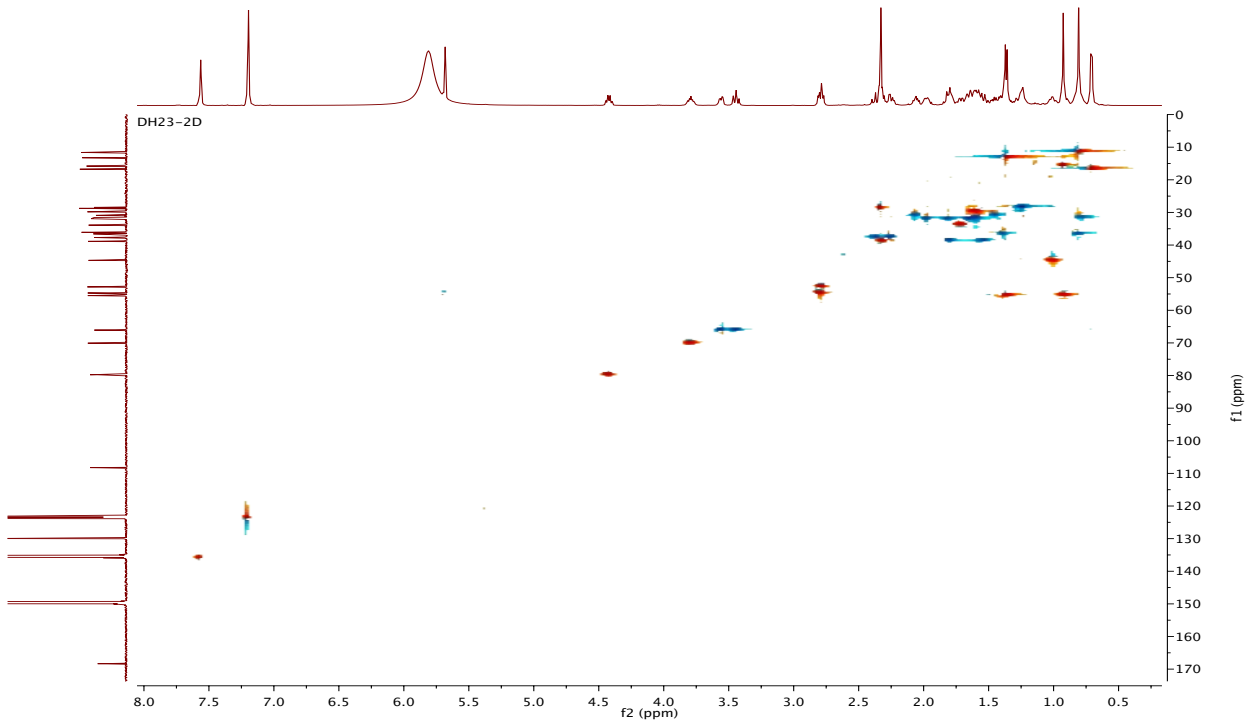


Figure S31. HSQC-NMR spectrum at 500 MHz in CDCl_3 of Bi-23-acetylhecogenin ester (**10b**).

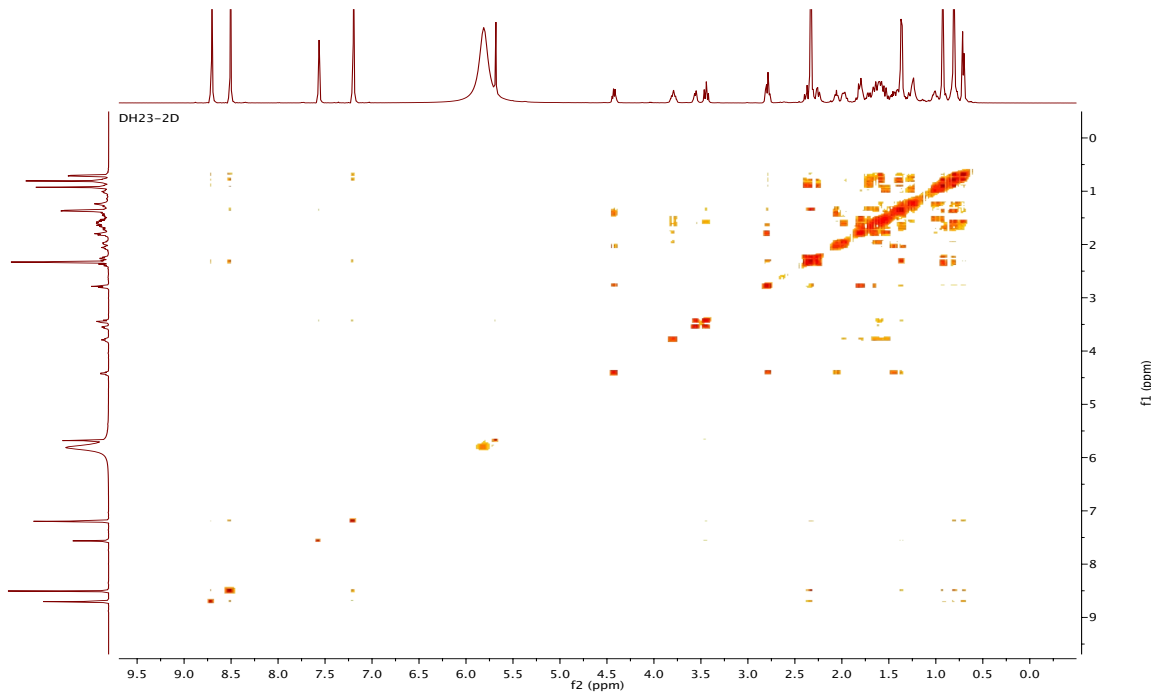


Figure S32. COSY-NMR spectrum at 500 MHz in CDCl_3 of Bi-23-acetylhecogenin ester (**10b**).

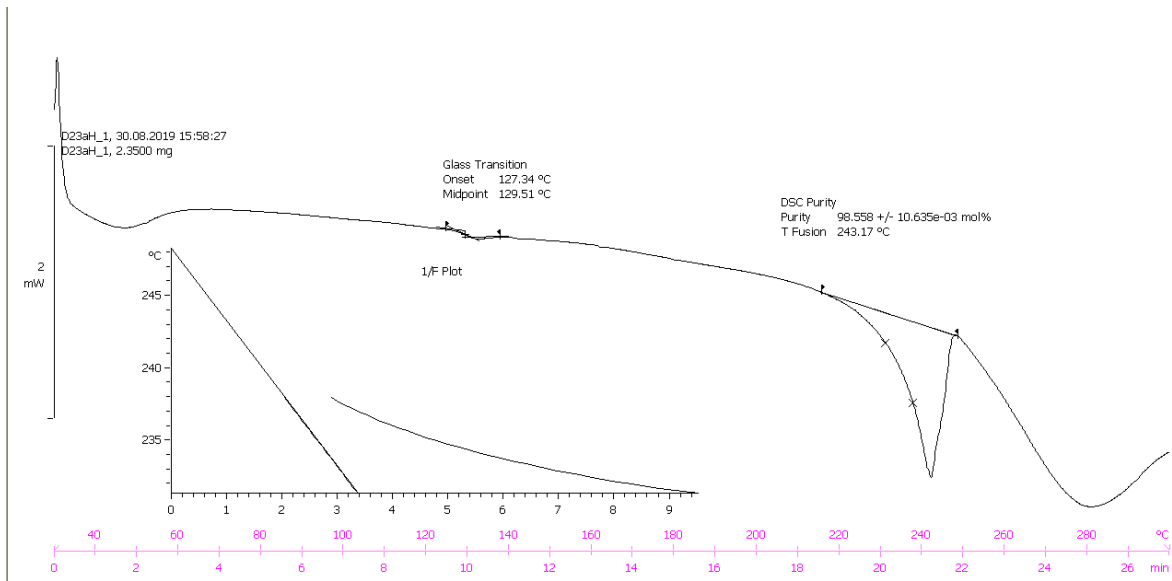


Figure S33. Differential Scanning Calorimetry analysis of Bi-23-acetylhecogenin ester (**10b**).

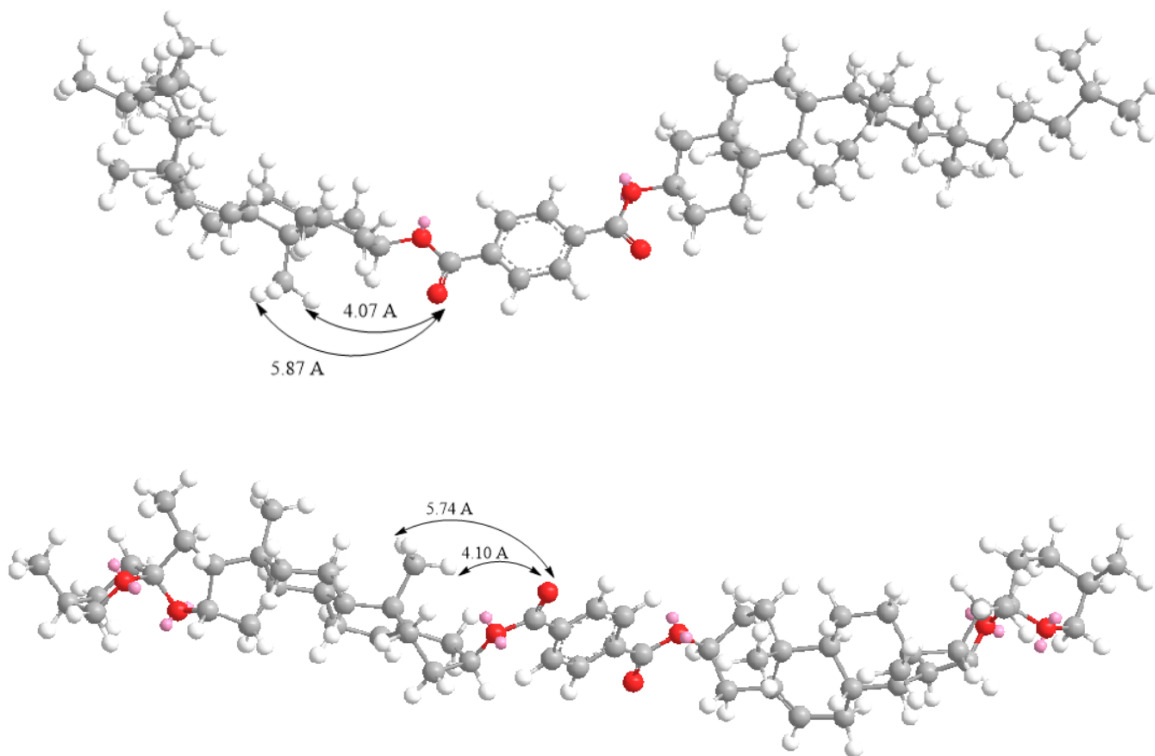


Figure S34. Molecular structure with MM2 energy minimization method for series: 5 α (**6**, top) and 5 β (**8c**, down).

Scanning Electron Microscopy (SEM) Images.

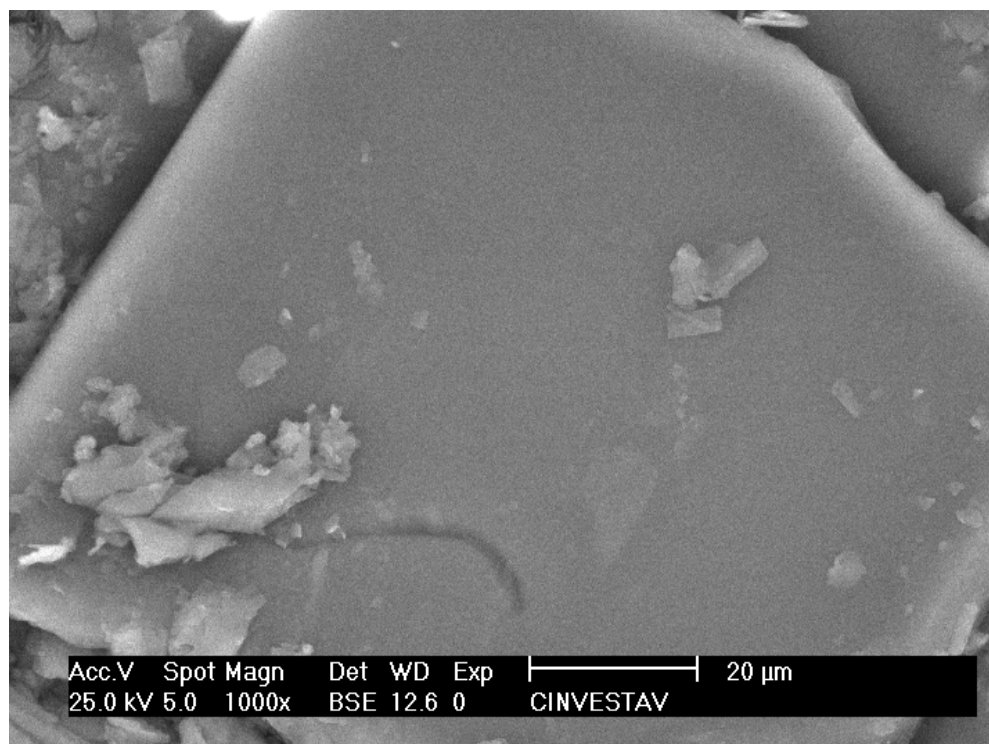


Figure S35 Bicholesterol ester (**5**) in hexane/ EtOAc showing membrane-shaped structures.

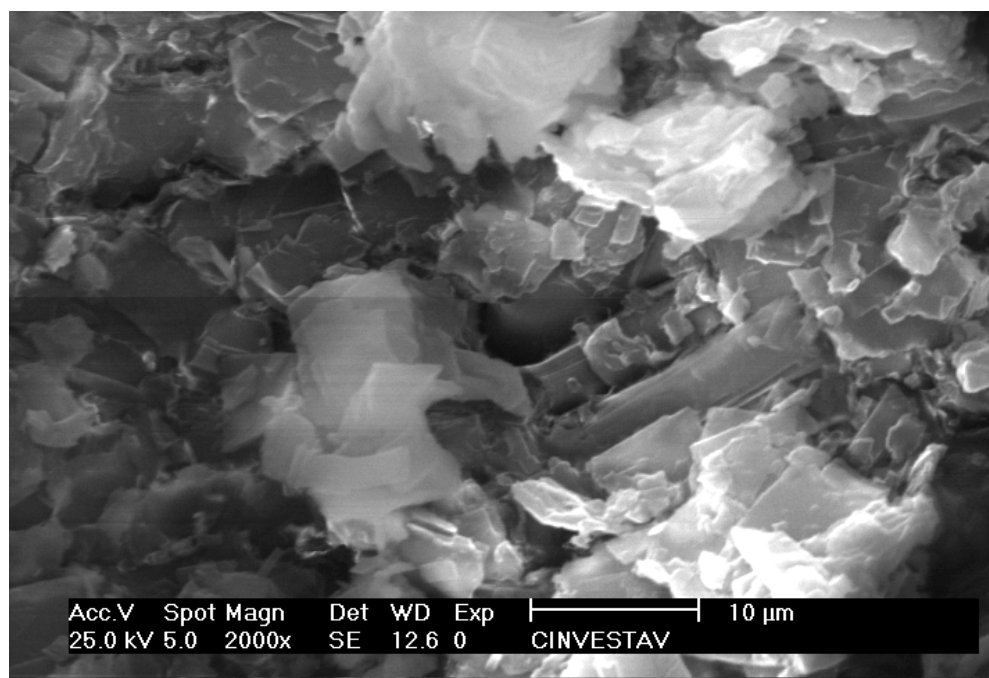


Figure S36 Bicholesterol ester (**5**) in hexane/ EtOAc showing membrane-shaped structures.

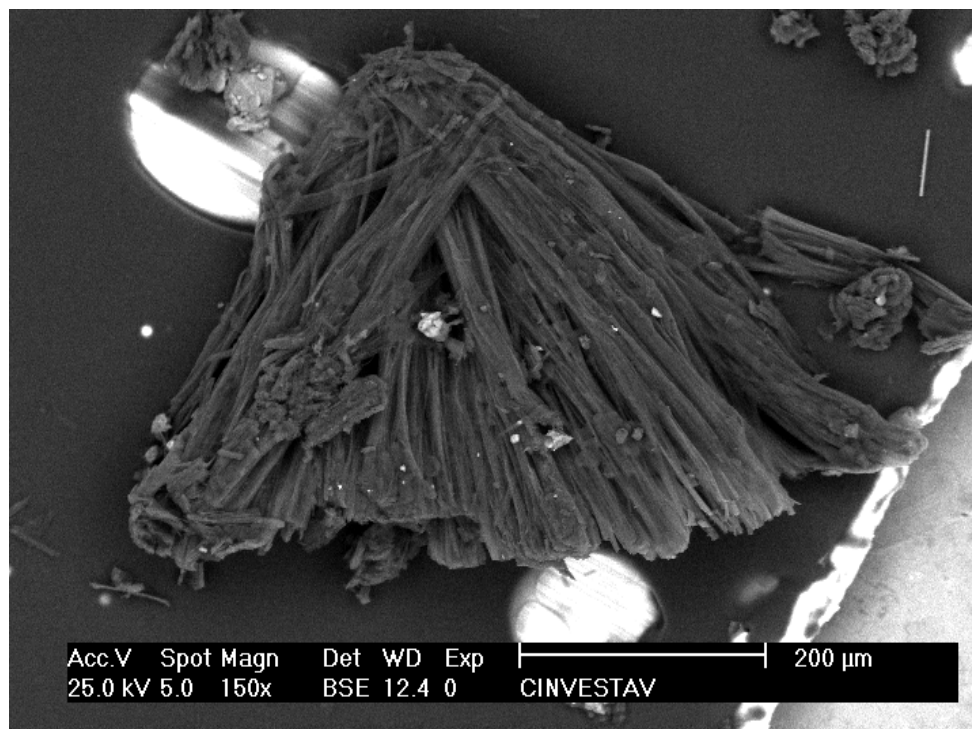


Figure S37. Bicholesterol ester (**5**) EtOAc showing strand-shaped structures.

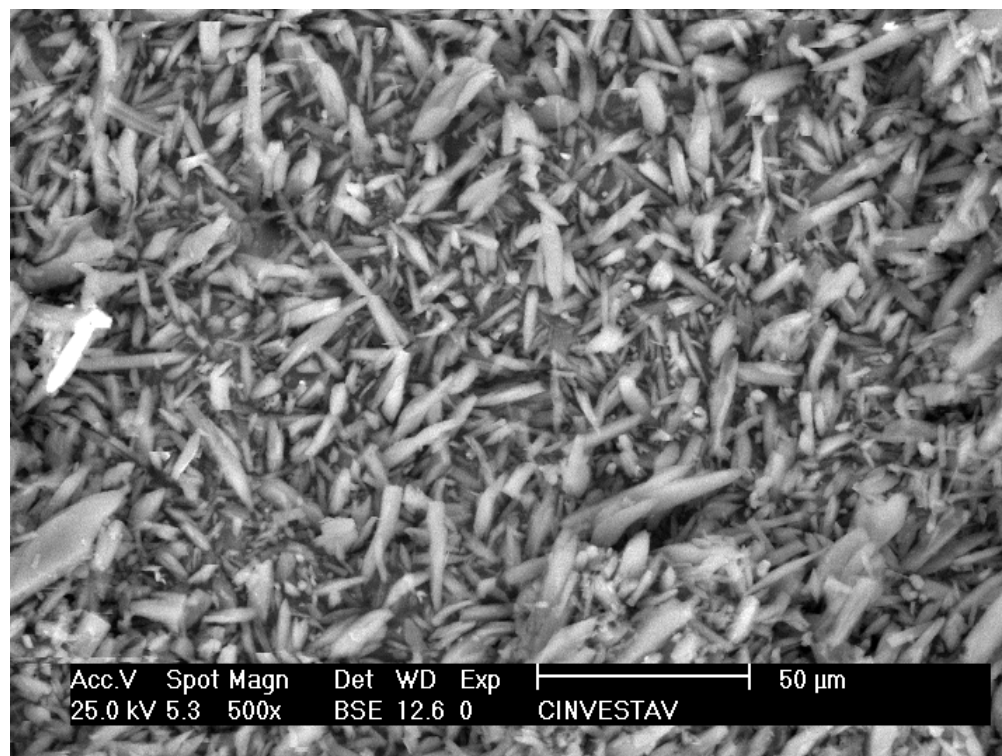


Figure S38. Bidiosgenin ester (**8a**) in EtOAc showing strand-shaped structures.

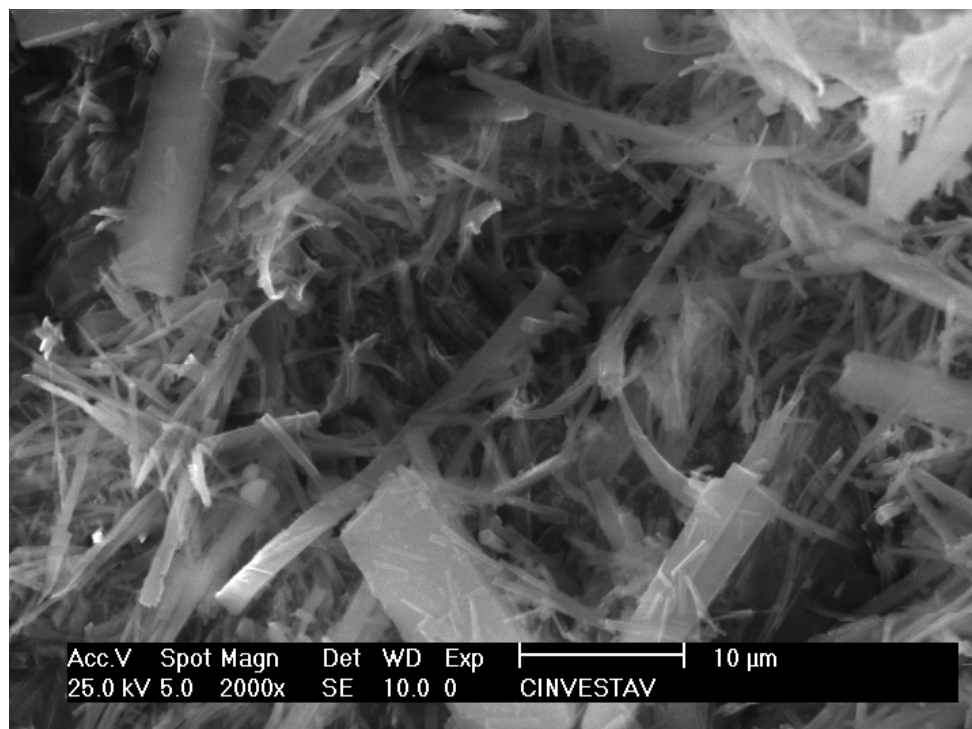


Figure S39. Bidiosgenin ester (**8a**) in CHCl₃/MeOH.

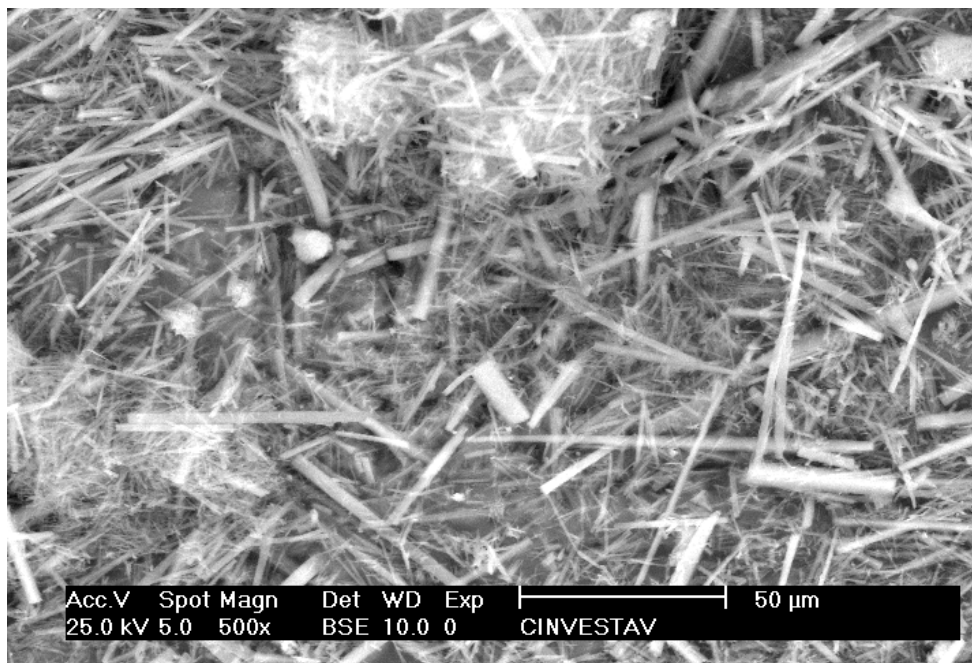


Figure S40. Bidiosgenin ester (**8a**) in CHCl₃/MeOH

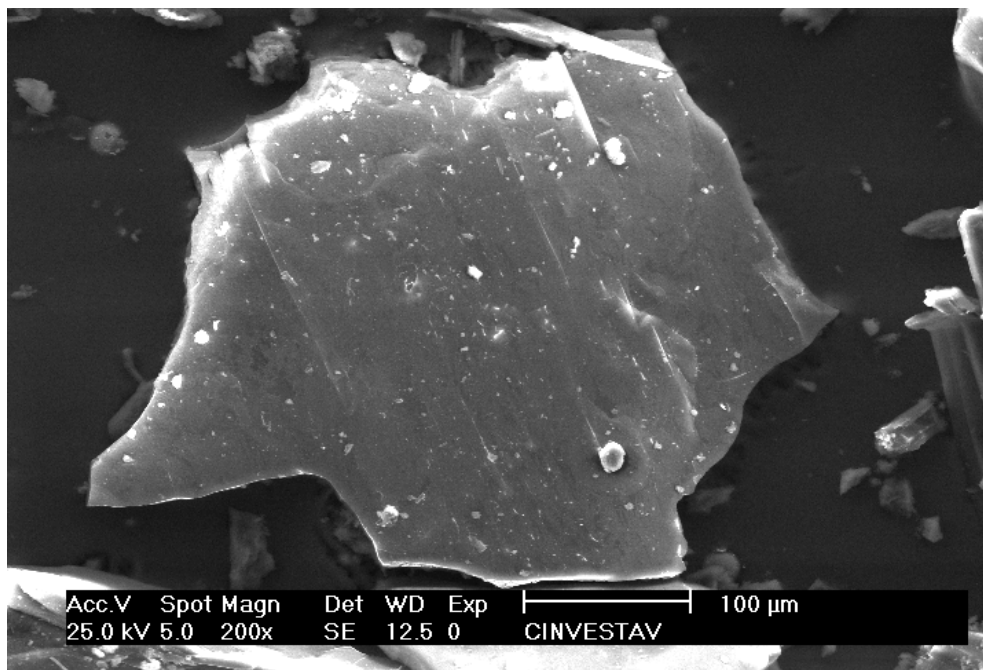


Figure S41. Bisarsasapogenin ester (**8c**) in hexane/EtOAc showing membrane-shaped structures.

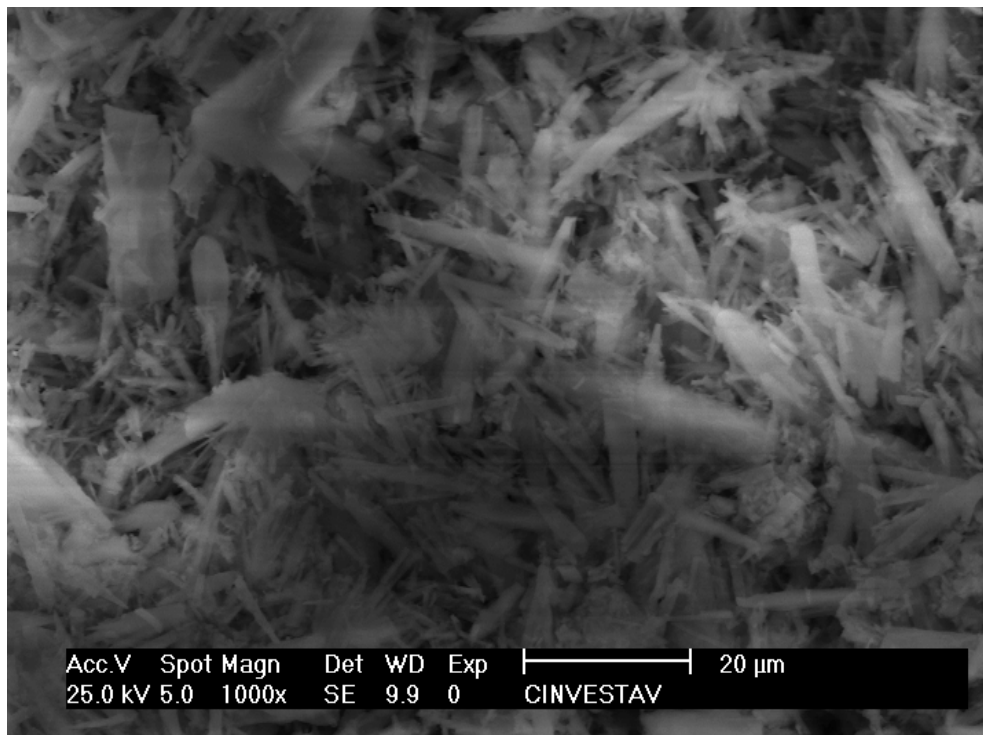


Figure S42. Bi-23-acetyldiosgenin ester (**10a**) in EtOAc showing strand-shaped structures.

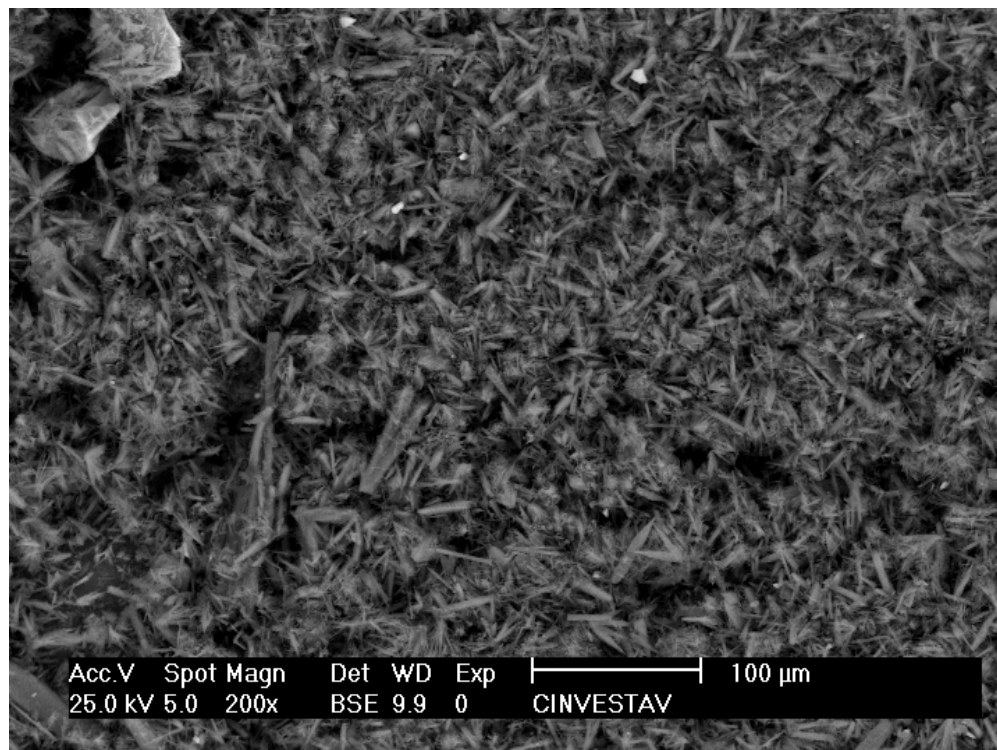


Figure S43. Bi-23-acetyldiosgenin ester (**10a**) in EtOAc showing strand-shaped structures.

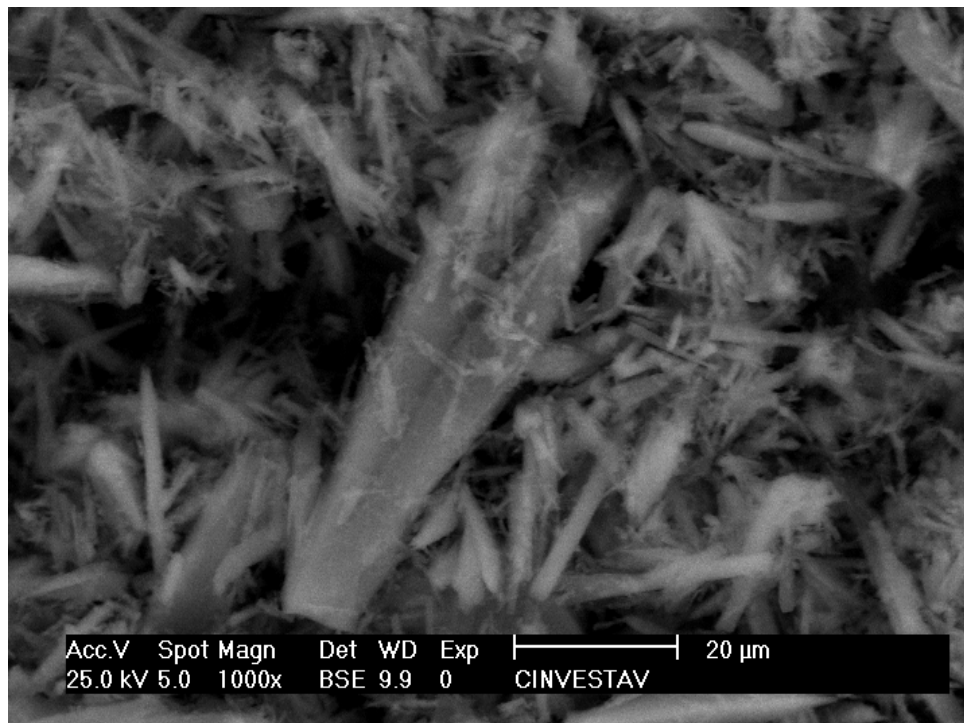


Figure S44. Bi-23-acetyldiosgenin ester (**10a**) in EtOAc showing strand-shaped structures.

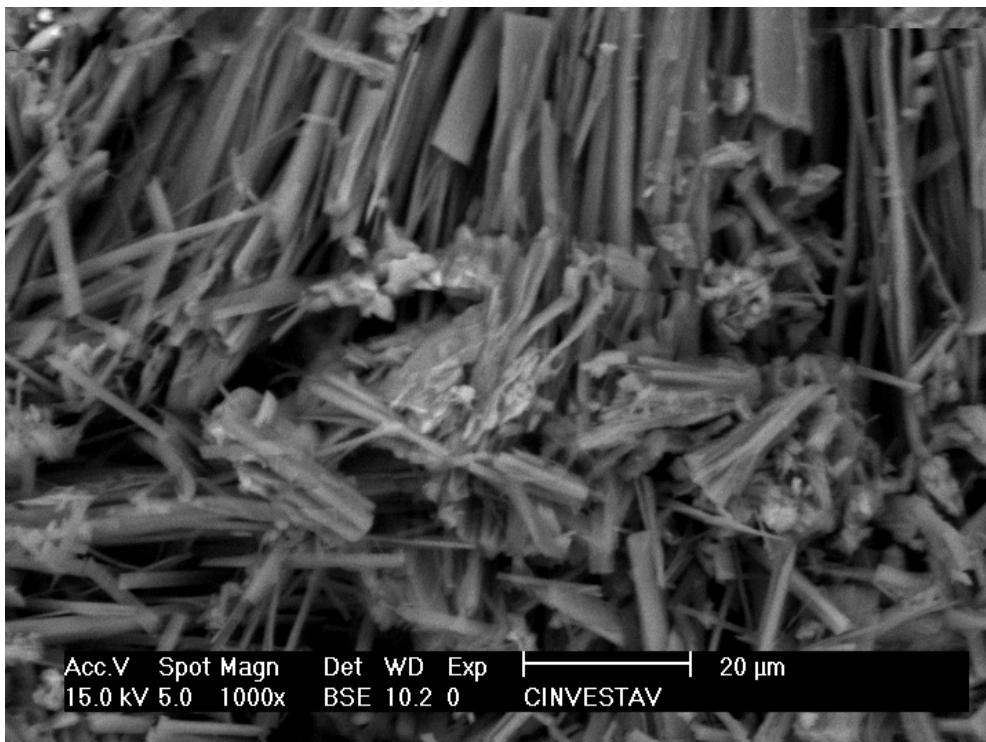


Figure S45. Bi-23-acetylhecogenin ester (**10b**) in EtOAc showing strand-shaped structures.

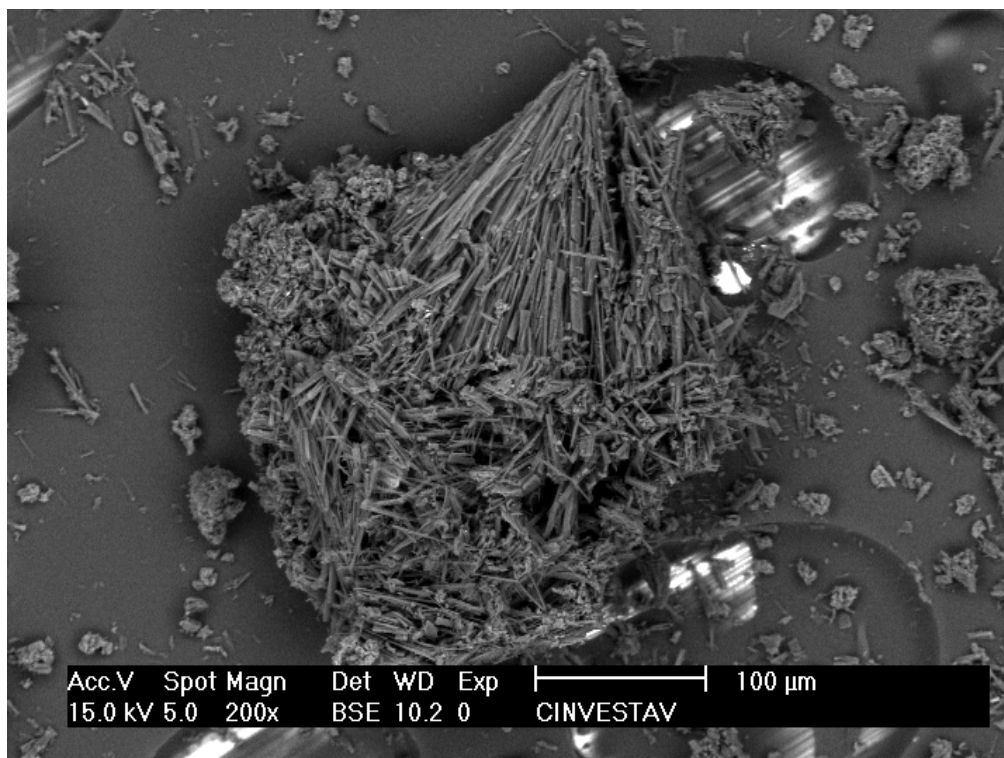


Figure S46. Bi-23-acetylhecogenin ester (**10b**) in EtOAc showing strand-shaped structures.

Powder X-ray diffraction (PXRD) analysis.

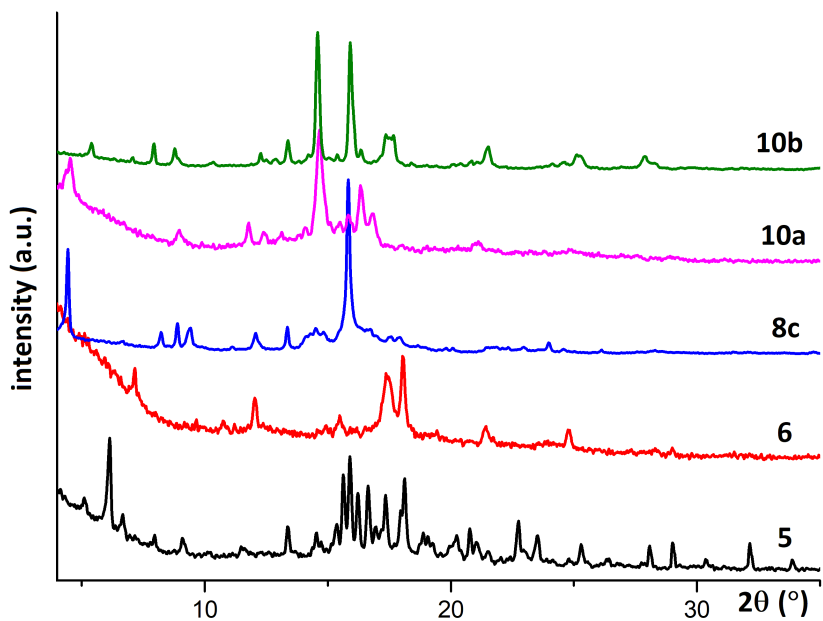


Figure S47. Powder X-ray diffraction patterns for raw materials of steroidal dimers **5**, **6**, **8c**, **10a** and **10b**. Patterns were collected with the Cu- $K\alpha$ radiation, and are uncorrected for amorphous contribution.

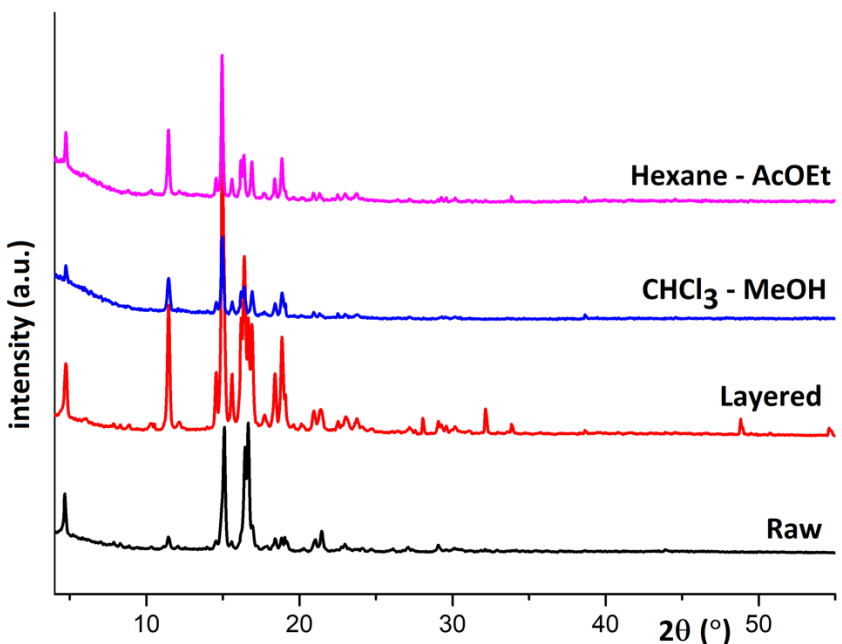


Figure S48. Comparison of the X-ray diffraction patterns of bidiosgenin ester (**8a**) under different conditions: raw material, layered material, dimer in contact with chloroform-methanol, and with hexane-ethyl acetate. Patterns were collected with the Cu- $K\alpha$ radiation, and are uncorrected for amorphous contribution. Note the intensity variation for the peak at $2\theta = 11.5^\circ$, as a consequence of the self-organization of the steroidal dimer.